Unraveling the critical indicators for evaluating the high-temperature performance of rejuvenator-aged bitumen blends

Ren, S.; Liu, X.; Erkens, S.

DOI
10.1016/j.cscm.2023.e02522

Publication date
2023

Document Version
Final published version

Published in
Case Studies in Construction Materials

Case Studies in Construction Materials 19 (2023) e02522

Contents lists available at ScienceDirect

Case Studies in Construction Materials

journal homepage: www.elsevier.com/locate/cscm

Unraveling the critical indicators for evaluating the high-temperature performance of rejuvenator-aged bitumen blends

Shisong Ren *, Xueyan Liu, Sandra Erkens

Section of Pavement Engineering, Faculty of Civil Engineering and Geosciences, Delft University of Technology, the Netherlands

ARTICLE INFO

Keywords:
High-temperature performance
Critical evaluation indicators
Rejuvenated bitumen
Rejuvenator type/dosage
Bitumen aging level

ABSTRACT

This study aims to systematically investigate the influence of rejuvenator type/dosage and the aging degree of bitumen on the rutting resistance, flow behavior, and elastic/creep potential of rejuvenated bitumen at high temperatures. The rutting parameter ($G^*/\sin\delta$), rutting failure temperature (RFT) from Linear viscoelastic test (LVE), zero-shear viscosity (ZSV) from flow test, recovery percentage ($R_{0.1}$, $R_{3.2}$), creep compliance ($J_{nr0.1}$, $J_{nr3.2}$), and stress sensitivity parameters (R_{diff}, $J_{nrslope}$) from multiple stress creep and recovery (MSCR) tests of rejuvenated bitumen are characterized. The results reveal that bio-oil rejuvenator weakens the high-temperature performance of aged bitumen maximally, followed by engine-oil and naphthenic-oil, while aromatic-oil rejuvenated bitumen exhibits the best rutting, flow, and creep resistance. The RFT index can most effectively evaluate and differentiate the rejuvenation efficiency of various rejuvenators on the high-temperature performance, which correlates well with ZSV, $R_{3.2}$, $J_{nr0.1}$, $J_{nr3.2}$, R_{diff}, and $J_{nrslope}$ indices. Therefore, the RFT index is recommended as the critical indicator for evaluating the high-temperature performance of rejuvenated binders. The flow and MSCR characteristics of rejuvenated bitumen can be predicted based on RFT values. The determination of critical indicators is beneficial to compare the rejuvenation effectiveness of variable rejuvenators on the high-temperature performance of aged bitumen.

1. Introduction

Presently, pavement researchers are increasingly focusing their efforts on circular and eco-friendly asphalt pavements, which involve the recycling of reclaimed pavement (RAP) waste materials [1–3]. However, the utilization of RAP is constrained by its diminished cracking resistance and adhesive properties [4,5]. This deficiency in RAP performance can be primarily attributed to the elevated stiffness and susceptibility to cracking of the aged bitumen it contains [6,7].

To facilitate the reutilization of RAP material, the pivotal focus revolves around mitigating the challenges associated with the low-temperature behavior and fatigue resistance of aged binders [8,9]. The incorporation of rejuvenators, also known as recycling agents, plays a crucial role in revitalizing and enhancing the chemical, rheological, morphological, and mechanical attributes of aged bitumen [10]. Zhang et al. conducted observations demonstrating the efficacy of sunflower oil in significantly enhancing the rheological properties, flow characteristics, and self-healing capabilities of aged bitumen [11–14]. Their findings also unveiled a connection

* Corresponding author.
E-mail address: Shisong.Ren@tudelft.nl (S. Ren).

https://doi.org/10.1016/j.cscm.2023.e02522
Received 4 July 2023; Received in revised form 2 September 2023; Accepted 1 October 2023
Available online 2 October 2023

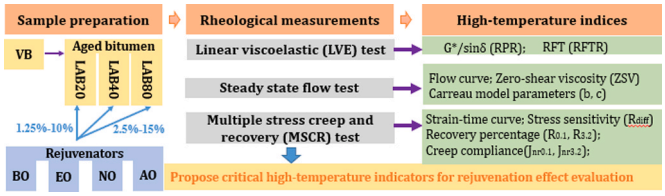

Fig. 1. Research protocol and roadmap.

between the thermal properties of rejuvenators and the rheological alterations in aged binders. Furthermore, it became evident that rejuvenators, even when sourced from the same origin, exhibited distinct behaviors [15,16].

There is a consensus that bitumen aging yields significant benefits by reinforcing the intermolecular bonds within the bitumen structure, consequently enhancing its resistance to high-temperature rutting and deformation [17,18]. Nonetheless, the introduction of rejuvenators composed of lighter constituents tends to soften the aged bitumen, thereby diminishing its high-temperature performance [19]. The guiding principle in the rejuvenation process is to strike a balance between the high-temperature and low-temperature properties of the rejuvenated bitumen [20,21]. Achieving this equilibrium necessitates the careful optimization of both the type and quantity of rejuvenators, with the goal of improving cracking resistance and adhesion performance while preserving the high-temperature characteristics of the aged bitumen [22–24]. The maximum allowable rejuvenator content is typically determined based on high-temperature performance criteria [25,26].

Nonetheless, the utilization of diverse assessment methods and criteria has resulted in challenges when attempting to directly compare the efficacy of various rejuvenators in enhancing the high-temperature characteristics of aged bitumen [27,28]. The SHARP project has introduced the rutting parameter (G*/sinδ) along with the corresponding rutting failure temperature as commonly employed indicators for assessing the rutting performance of bituminous materials [29]. Recent research has shown that the multiple stress creep and recovery (MSCR) test can provide better differentiation among complex bitumen samples compared to traditional indicators [30]. However, Skronka et al. discovered that the MSCR test tended to overestimate the favouable impact of elasticity on the high-temperature rutting performance of asphalt mixtures [31]. Furthermore, Sharma et al. noted a strong correlation between the zero-shear viscosity measured in flow tests and the high-temperature rutting performance of asphalt bitumen and mixtures [32].

Following the examination of existing literature, several limitations in the assessment of high-temperature performance for rejuvenated bitumen become evident:

(a) A lack of a standardized methodology and a uniform set of criteria exist for evaluating the high-temperature characteristics of bituminous materials.
(b) The composition disparity in rejuvenator-aged bitumen blends exerts a substantial influence on high-temperature performance. Unfortunately, there is a scarcity of comprehensive research dedicated to systematically exploring and contrasting the effectiveness of various rejuvenators in enhancing the high-temperature behavior of aged bitumen.
(c) The potential relationships among diverse rheological indicators pertaining to high temperatures in rejuvenated bitumen remain poorly understood.

2. Objective and methodology

The main objective of this study is to explore the influence of aging and rejuvenation conditions on the high-temperature deformation resistance of bitumen with various rheological methods and propose the critical indicators for evaluating the rejuvenation effects of various rejuvenators on the high-temperature performance of aged bitumen. Compared to prior research, this study introduces a systematic approach to identify crucial high-temperature assessment criteria for rejuvenated bitumen, considering various factors of rejuvenator type/dosage and bitumen aging degree. Fig. 1 illustrates the research roadmap. First, different aged bitumen and rejuvenators would be blended with variable rejuvenator dosages to prepare a series of rejuvenated binders. Afterward, three commonly-used high-temperature rheological tests (linear viscoelastic, steady-state flow, and multiple stress creep and recovery) will be conducted to assess the effects of rejuvenator type/dosage and aging level of bitumen on the high-temperature rutting, flow, and resilience behaviors of rejuvenated bitumen. Different evaluation indicators from these tests will be considered to quantitatively reflect the rejuvenation efficiency on the high-temperature performance of various rejuvenator-aged bitumen blends. By comparing the sensitivity of these evaluation indices to the changeable aging/rejuvenation conditions, the critical high-temperature indicators for rejuvenation effect evaluation will be recommended. Lastly, the potential connections between these proposed critical indicators from different tests will be disclosed.

3. Materials and characterization tests

3.1. Bitumen and rejuvenators

A bitumen from one European petrochemical company with 70/100 penetration grade was used as the fresh bitumen (VB). The conventional properties, saturate, aromatic, resin, and asphaltene (SARA) fractions of fresh bitumen are listed in Table 1. It should be

Table 1
The conventional indices and chemical components of 70/100 fresh bitumen.

Properties	Value	Specification
25 ℃ Density (g·cm^{-3})	1.017	EN 15326 [35]
25 ℃ Penetration (0.1 mm)	91	ASTM D35 [36]
Softening point (℃)	48.0	ASTM D36 [37]
135 ℃ Viscosity (Pa·s)	0.80	AASHTO T316 [38]
Saturate content (wt%)	3.6	ASTM D4121 [39]
Aromatic content (wt%)	53.3	
Resin content (wt%)	30.3	
Asphaltene content (wt%)	12.8	

Table 2
The physical and chemical properties of four rejuvenators.

Properties	Bio-oil	Engine-oil	Naphthenic-oil	Aromatic-oil
25 ℃ Density (g·cm^{-3})	0.911	0.833	0.875	0.994
25 ℃ Viscosity (cP)	50	60	130	63100
Flash point (℃)	265–305	> 225	> 230	> 210
Average weight Mn (g·mol^{-1})	286.43	316.48	357.06	409.99
Carbon content (wt%)	76.47	85.16	86.24	88.01
Hydrogen content (wt%)	11.96	14.36	13.62	10.56
Sulfur content (wt%)	0.06	0.13	0.10	0.48
Oxygen content (wt%)	11.36	0.12	0.10	0.40
Nitrogen content (wt%)	0.15	0.23	0.12	0.55

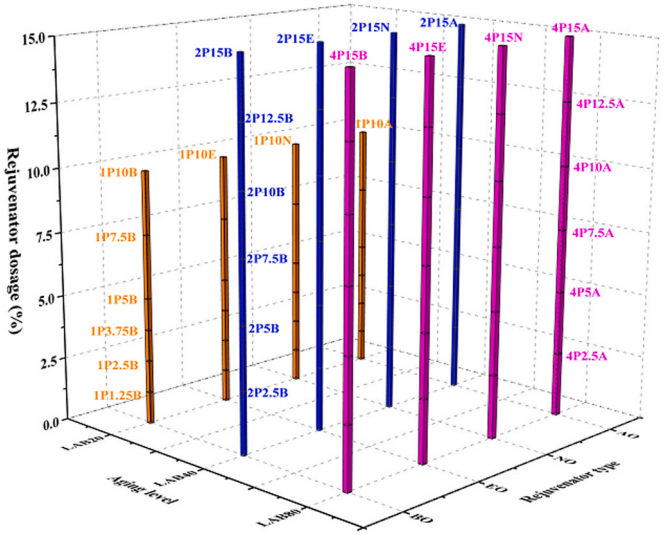

Fig. 2. The 76 kinds of rejuvenated bitumen involved in this study.

mentioned that this work mainly concentrates on the rejuvenation efficiency evaluation of various rejuvenator-aged bitumen blends with changeable aging levels and rejuvenator type/dosage, but the influence factor of bitumen type is not considered herein.

Table 2 displays the physical properties, average weight, and elemental components of selected rejuvenators: Bio-oil (BO), Engine-oil (EO), naphthenic-oil (NO), and aromatic-oil (AO) [33]. These rejuvenators are chosen based on the America National Center for Asphalt Technology (NCAT) recommendation [34]. It is found that the different rejuvenators exhibit differences in both physical and chemical properties. For example, the bio-oil shows the lowest viscosity and molecular weight and highest oxygen dosage, which is limited in the other three rejuvenators. Additionally, the aromatic-oil has the largest density, viscosity, Mn, and C/H ratio. All these physiochemical differences of rejuvenators will contribute to their different rejuvenation efficiency on the high-temperature performance of aged bitumen.

3.2. Preparation of aged and rejuvenated bitumen

The artificial long-term aged bitumen was prepared in the laboratory by combining the Thin film oven test (TFOT) and pressure

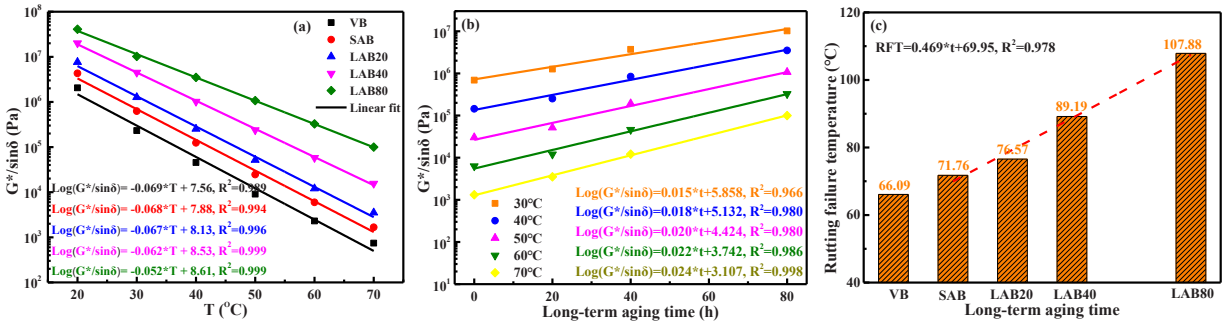

Fig. 3. Rutting characteristics of fresh and aged bitumen.

aging vessel (PAV) test for the short-term and long-term aging process of bitumen, respectively. The aging time and temperature of TFOT are 5 h and 163 ℃. Meanwhile, the PAV tests were implemented under the temperature and pressure condition of 100 ℃ and 2.1 MPa. Different PAV aging times of 20, 40, and 80 h were adopted to obtain the aged binders with discriminative aging degrees. In this study, fresh bitumen, short-term aged bitumen, and long-term aged bitumen with 20, 40, and 80 h were abbreviated as VB, SAB, LAB20, LAB40, and LAB80.

All rejuvenated binders were prepared with the same manufacturing process to eliminate their influence on high-temperature performance evaluation. The aged bitumen was preheated at 160 ℃ for 30 min to reach a flow state, and the rejuvenator was blended in aged bitumen by a mixer at 160 ℃ for 10 min to prepare the homogeneous rejuvenated bitumen. Fig. 2 presents detailed information on all rejuvenated binders, including the rejuvenator dosage, rejuvenator type, and aging level of bitumen. To the LAB20 aged bitumen (slight aging), the rejuvenator content is 1.25%, 2.5%, 3.75%, 5%, 7.5%, and 10%. Meanwhile, the rejuvenator dosage scopes for LAB40 and LAB80 are the same, varying from 2.5% to 15% with an interval of 2.5%. Further, the abbreviations of these rejuvenated bitumen are also shown in Fig. 2, composed of aging degree, rejuvenator dosage, and rejuvenator type. For instance, the 2P15B means that rejuvenated bitumen is prepared by mixing the 15 wt% bio-oil rejuvenator in LAB40 aged bitumen.

3.3. Linear viscoelastic (LVE) rutting test

All high-temperature tests on bitumen samples are implemented using a dynamic shear rheometer (DSR) with the specimen size of 25 mm diameter and 2 mm thickness. The temperature sweep test measures the variation trend of rutting parameter in the linear viscoelastic region. The temperature rises from 30 ℃ to 70 ℃, with an interval of 10 ℃. The frequency during the LVE test is constant at 10 rad/s [40]. All experimental measurements were conducted with at least two replicates to achieve reliable results.

3.4. Steady state flow test

The zero-shear viscosity (ZSV) is closely related to the rutting potential of the asphalt binder and mixture [41]. The flow test at different temperatures of 40 ℃, 50 ℃, and 60 ℃ was implemented with DSR to measure the difference in flow behavior and ZSV index of various rejuvenator-aged bitumen blends. The shear rate of all flow tests varies from 10^{-3} s^{-1} to 10^{2} s^{-1} [42]. The viscosity-shear strain flow curves will be obtained to estimate the effects of aging and rejuvenation on the bitumen's high-temperature shear characteristic and resistance.

3.5. Multiple stress creep and recovery (MSCR) test

The MSCR tests were performed at two stress levels of 0.1 kPa and 3.2 kPa at different temperatures of 52 ℃, 58 ℃, 64 ℃, and 70 ℃, respectively [43]. Ten cycles (a total time of 200 s) were included in the MSCR test at each applied stress level. The bitumen specimen experienced 1 s creep and 9 s recovery stages for each cycle. The strain-time response was monitored (as shown in Fig. 3), and two rheological indices (non-recoverable creep compliance J_{nr} (kPa^{-1}) and recovery percentage R (%)) can be calculated as follows:

$$\mathrm{Jnr}(\sigma, \mathrm{N}) = \frac{\varepsilon_r - \varepsilon_c}{\sigma} \tag{1}$$

$$\mathrm{R}(\sigma, \mathrm{N}) = \frac{\varepsilon_c - \varepsilon_r}{\varepsilon_c - \varepsilon_0} \times 100 \tag{2}$$

where σ and N refer to the applied stress (kPa) and the creep/recovery cycles; ε_r (%) and ε_r (%) are the shear strain value measured at the end of creep and recovery steps, respectively; ε_0 (%) represents the initial shear strain in the creeping stage. The J_{nr} parameter is related to the deformation potential of bituminous material, while the R index reflects the resilience. Eqs.3–5 show the R and Jnr parameters at both 0.1 kPa and 3.2 kPa stress levels.

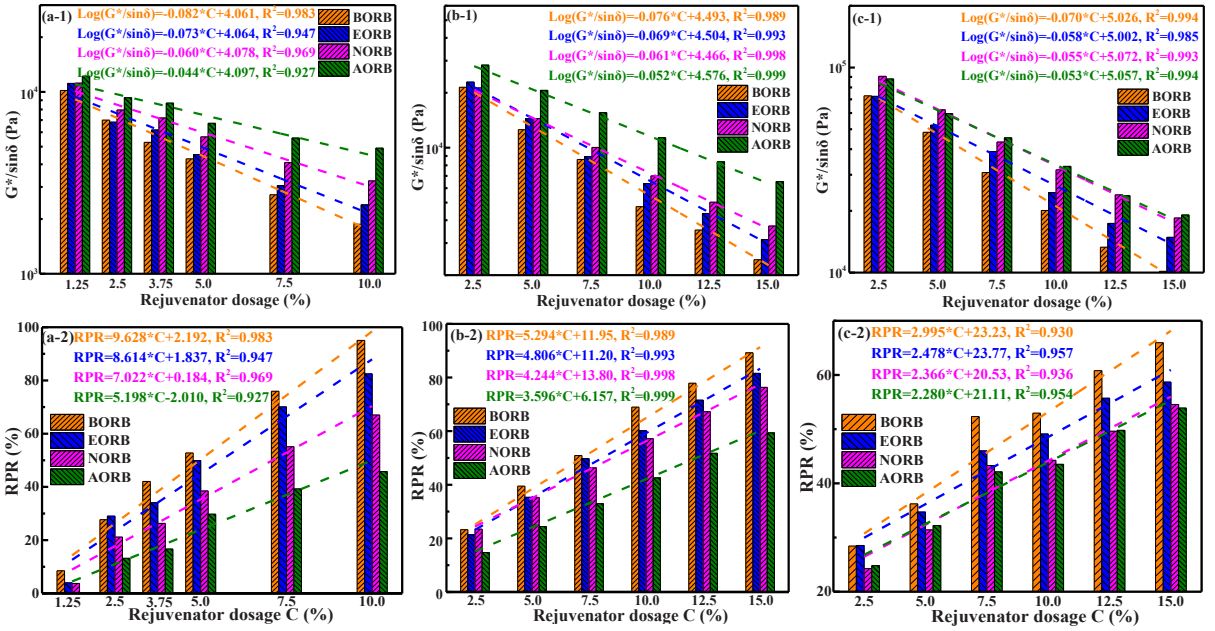

Fig. 4. The G* /sinδ and RPR values of rejuvenated bitumen at 60 ℃. (a) LAB20, (b) LAB40, and (c) LAB80.

$$R_{0.1} = \frac{\sum_{N=11}^{20} R(0.1, N)}{10} \tag{3}$$

$$J_{nr0.1} = \frac{\sum_{N=11}^{20} J_{nr}(0.1, N)}{10} \tag{4}$$

$$R_{3.2} = \frac{\sum_{N=1}^{10} R(3.2, N)}{10} \tag{5}$$

$$J_{nr3.2} = \frac{\sum_{N=1}^{10} J_{nr}(3.2, N)}{10} \tag{6}$$

The MSCR results are strongly sensitive to the stress level, and two parameters ($J_{nrslope}$ and R_{diff}) are calculated to assess the dependence of fresh, aged, and rejuvenated bitumen on the stress applied using Eqs.7 and 8.

$$J_{nrslope} = \frac{dJ_{nr}}{d\sigma} = \frac{J_{nr3.2} - J_{nr0.1}}{3.1} \times 100 \tag{7}$$

$$R_{diff} = \frac{R_{3.2} - R_{0.1}}{R_{0.1}} \times 100 \tag{8}$$

where stress differential dσ equals 3.1 kPa; $J_{nr3.2}$ and $J_{nr0.1}$ are the creep compliance of bitumen at the stress of 3.2kPa and 0.1kPa, while the $R_{3.2}$ and $R_{0.1}$ are the corresponding recovery percentages.

4. Results and discussion

4.1. Rutting potential from LVE test

The rutting parameter G* /sinδ of fresh and aged bitumen are displayed in Fig. 3 at different temperatures of 30 ℃, 40 ℃, 50 ℃, 60 ℃ and 70 ℃. The influence of temperature and long-term aging time on the rutting potential of bitumen is investigated. The G* /sinδ value of bitumen tends to decrease linearly as the temperature rise, indicating that the rutting potential is larger at higher temperatures. This occurs because bitumen molecules exhibit increased molecular mobility and reduced intermolecular forces when exposed to high temperatures. The aging degree of bitumen significantly reduces the absolute slope values of G* /sinδ-T curves,

Table 3
Correlation parameters of RPR-C curves.

Aging level	T (℃)	Samples	k	b	R^2	Samples	k	b	R^2
LAB20	30	BORB	11.074	8.987	0.982	NORB	7.974	4.033	0.966
	40		10.495	7.483	0.982		7.484	4.766	0.970
	50		9.848	5.016	0.970		7.194	1.423	0.964
	60		9.628	2.192	0.983		7.022	0.184	0.969
	70		9.366	4.971	0.970		7.063	1.372	0.940
	30	EORB	10.050	5.320	0.961	AORB	5.354	-1.84	0.991
	40		9.220	6.310	0.946		5.083	1.661	0.969
	50		8.870	3.790	0.957		5.368	-1.06	0.949
	60		8.610	1.840	0.947		5.198	-2.01	0.927
	70		8.520	4.490	0.942		5.464	-0.02	0.934
LAB40	30	BORB	6.365	17.095	0.978	NORB	4.897	16.170	0.998
	40		5.704	16.658	0.983		4.624	15.770	0.997
	50		5.343	14.280	0.989		4.358	14.460	0.998
	60		5.294	11.952	0.989		4.244	13.800	0.988
	70		5.287	11.392	0.988		4.349	13.460	0.998
	30	EORB	5.410	15.260	0.990	AORB	3.456	6.809	0.997
	40		4.870	15.230	0.990		3.589	7.778	0.998
	50		4.800	12.340	0.993		3.553	7.558	0.994
	60		4.810	11.200	0.993		3.596	6.157	0.999
	70		4.980	10.200	0.993		3.674	6.063	0.998
LAB80	30	BORB	4.250	19.271	0.963	NORB	3.012	17.030	0.937
	40		3.602	22.947	0.951		2.598	20.840	0.932
	50		3.229	22.757	0.951		2.340	21.220	0.921
	60		2.995	23.233	0.931		2.344	20.720	0.914
	70		2.960	24.014	0.917		2.349	21.780	0.909
	30	EORB	3.330	20.300	0.927	AORB	2.369	14.810	0.915
	40		2.800	23.890	0.919		2.327	19.780	0.927
	50		2.560	23.580	0.939		2.268	20.690	0.936
	60		2.480	23.770	0.957		2.280	21.110	0.954
	70		2.440	24.710	0.947		2.383	21.770	0.962

showing that a high aging level decreases the temperature sensitivity of rutting performance. Meanwhile, the linearly increasing correlations between the G* /sinδ and long-term aging time are detected, regardless of the temperature. This suggests that bitumen's resistance to rutting significantly increases as it undergoes prolonged aging, a phenomenon attributed to the heightened stiffness and improved intermolecular interactions within aged bitumen. Moreover, the influence of aging time on G* /sinδ becomes more obvious at high temperatures. It means that the aging effect on the rutting performance of bitumen depends on the testing temperature.

Based on the SHARP recommendation, the rutting failure temperature (RFT) index is proposed to evaluate the rutting resistance of bitumen, which is the temperature when the G* /sinδ value is equivalent to 1000 Pa. The RFT results of fresh and aged bitumen are shown in Fig. 3**(c)**. As the long-term aging time prolongs from 0 to 20, 40, and 80 h, the RFT value of bitumen increases from 71.76 ℃ to 76.57 ℃, 89.19 ℃, and 107.88 ℃. The linear relationship between the RFT and aging time is beneficial to predict the RFT value of aged bitumen with other aging degrees.

To quantitively estimate the rejuvenation effect of rejuvenators on the high-temperature performance of aged bitumen, the rejuvenation percentage parameter is proposed based on different high-temperature indices as Eq.9.

$$PR = \frac{P_{aged} - P_{rejuvenated}}{P_{aged} - P_{fresh}} * 100 \quad (9)$$

where PR is the rejuvenation percentage, and P represents the high-temperature indices in Fig. 1. Meanwhile, the P_{fresh}, P_{aged}, and $P_{rejuvenated}$ are the high-temperature indices of fresh, aged, and rejuvenated binders, respectively.

Fig. 4 displays the rutting parameter and corresponding rejuvenation percentage RPR of rejuvenated bitumen at 60 ℃. Regardless of rejuvenator type and aging degree of bitumen, the Log(G*/sinδ) values of all rejuvenated binders tend to decrease linearly as the increased rejuvenator dosage, while the RPR parameter rises linearly. This suggests that the introduction of rejuvenators diminishes the high-temperature rutting resistance of aged bitumen due to their softening impact. The ranking of G* /sinδ values of rejuvenated bitumen is AORB > NORB > EORB > BORB, while the order of RPR values shows an opposite trend. Hence, the bio-oil rejuvenator exhibits the most pronounced reduction in the rutting resistance of aged bitumen, whereas the aromatic-oil effectively preserves its high-temperature performance advantage to the maximum extent. It is observed that the RPR values of all rejuvenated binders are lower than 100%, indicating that the anti-rutting performance of rejuvenated bitumen is still better than fresh bitumen. However, the rejuvenator dosage has to be controlled to ensure sufficient rutting resistance at high temperatures of rejuvenated bitumen, especially for bio-oil and engine-oil rejuvenators.

In addition, the G* /sinδ values of rejuvenated bitumen intensify significantly as the aging level of bitumen deepens, while the RPR parameter shows a reduction trend. Consequently, the effectiveness of rejuvenation in revitalizing the rutting resistance of highly aged bitumen decreases. It is intriguing that there is no discernible disparity in both G* /sinδ and RPR values between NORB and AORB

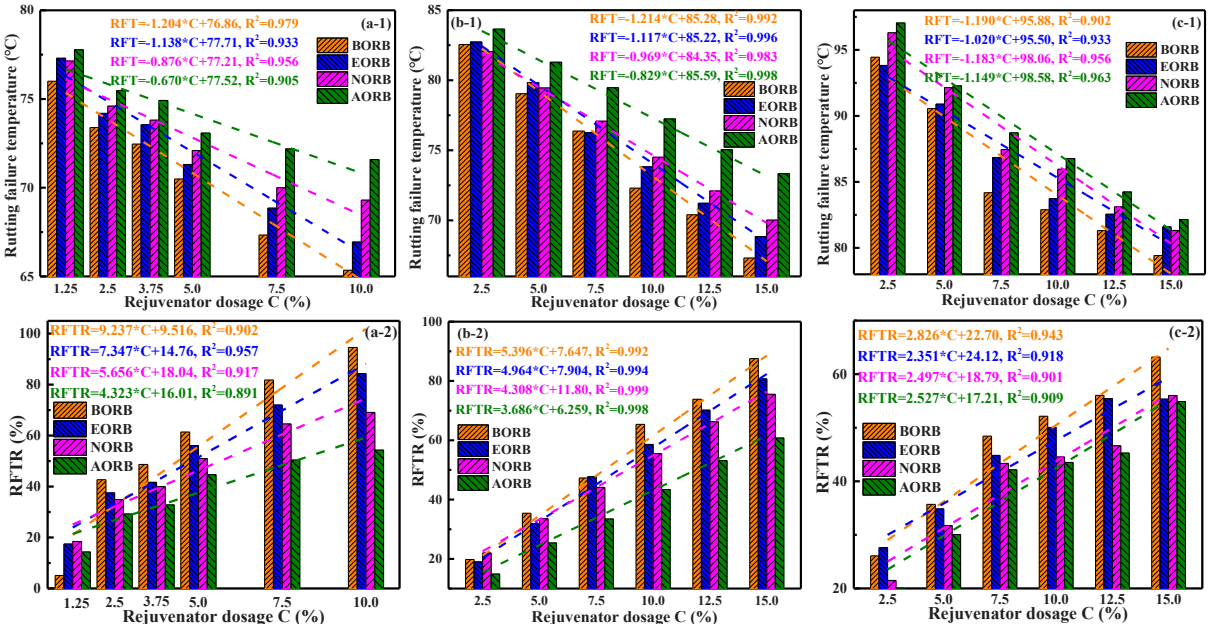

Fig. 5. Influence of rejuvenator dosage, type, and aging level on rutting failure temperature of rejuvenated bitumen (a) LAB20, (b) LAB40, and (c) LAB80.

binders. This can be attributed to the robust intermolecular interactions among LAB80 bitumen molecules and the limited softening capacity of naphthenic-oil and aromatic-oil. It is worth mentioning that the rejuvenation effect of these four rejuvenators on the rutting performance of aged bitumen can be effectively evaluated and distinguished by the G* /sinδ result. However, the rejuvenation percentage result is strongly dependent on the temperature.

To explore the impact of temperature, Table 3 summarizes the correlation parameters of RPR-C curves of different rejuvenated binders at variable testing temperatures. As the temperature increases, the k and b values decrease significantly, suggesting that elevated temperatures result in diminished rutting resistance and a reduced capacity of rejuvenators to enhance the high-temperature performance of aged bitumen. However, the temperature influences the sensitivity level of the RPR value to rejuvenator dosage becomes smaller when the temperature exceeds 50 ℃. Moreover, the rejuvenator type and aging degree of bitumen affect the temperature sensitivity of k and b parameters. The RPR values of BORB and EORB exhibit more sensitivity to temperature variation than the NORB and AORB. Additionally, the temperature susceptibility of RPR-C curves of rejuvenated bitumen weakens as the aging level of bitumen deepens.

The random selection of LVE temperature would result in the difference in rejuvenation percentages based on the G* /sinδ parameter. To eliminate the temperature effect, the rutting failure temperature (RFT) index is calculated with the G* /sinδ= 1.0kPa criteria [43], and the RFT-based rejuvenation percentages (RFTR) are obtained following Eq. 9. The results are displayed in Fig. 5. Similar to G* /sinδ, the RFT and RFTR show the linearly decreasing and increasing trend as the rejuvenator dosage rises, respectively. It is worth noting that the difference in both RFT and RFTR values of different rejuvenated binders is significant, regardless of the rejuvenator dosage and aging level of bitumen. The RFT index proves to be a more suitable choice for assessing and distinguishing the high-temperature rutting resistance among diverse blends of rejuvenator-aged bitumen, considering variations in rejuvenator type, dosage, and bitumen aging degree. As such, the RFT index is strongly recommended as an effective indicator for characterizing the high-temperature performance of rejuvenated bitumen.

4.2. Shear resistance from flow test

While the G* /sinδ and RFT parameters obtained from the LVE test are capable of illustrating and distinguishing the impact of various rejuvenators on the rutting resistance of aged bitumen, the strain levels involved are relatively small, and the entire LVE region lacks realistic deformation. Consequently, a flow test is conducted to assess the shear resistance of bituminous materials under varying conditions of aging and rejuvenation. The flow curves of fresh and aged bitumen are illustrated in Fig. 6(a). As observed, the flow behavior of bitumen strongly depends on the shear rate. Due to the Newtonian-flow characteristic, the complex viscosity remains constant at a low shear rate ($<1\ s^{-1}$). As the shear rate exceeds the critical point, the viscosity of bitumen decreases significantly as the shear rate rises. At this time, the bitumen is a non-Newtonian fluid.

Moreover, long-term aging exhibits a distinct effect on the complex viscosity and flow behavior of bitumen. As the aging level deepens, the viscosity of bitumen remarkably intensifies. Meanwhile, the Newtonian-fluid region shortens gradually. The Carreau model is adopted to quantitatively describe the flow curves of fresh, aged, and rejuvenated binders, which is defined as:

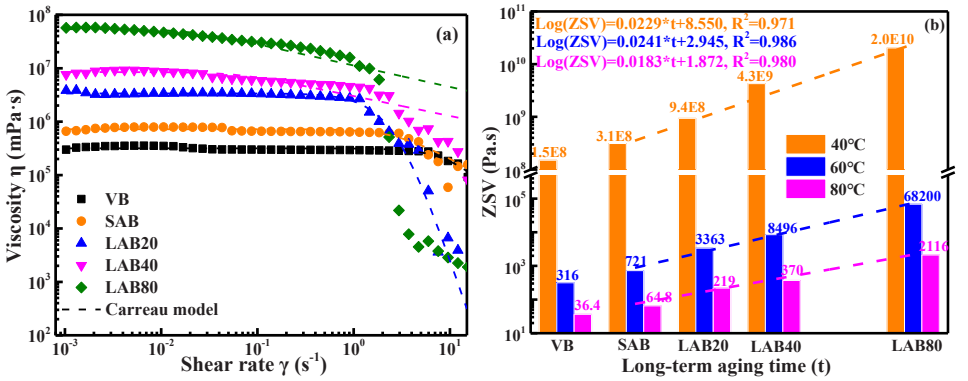

Fig. 6. Influence of aging on flow behavior and ZSV value of bitumen.

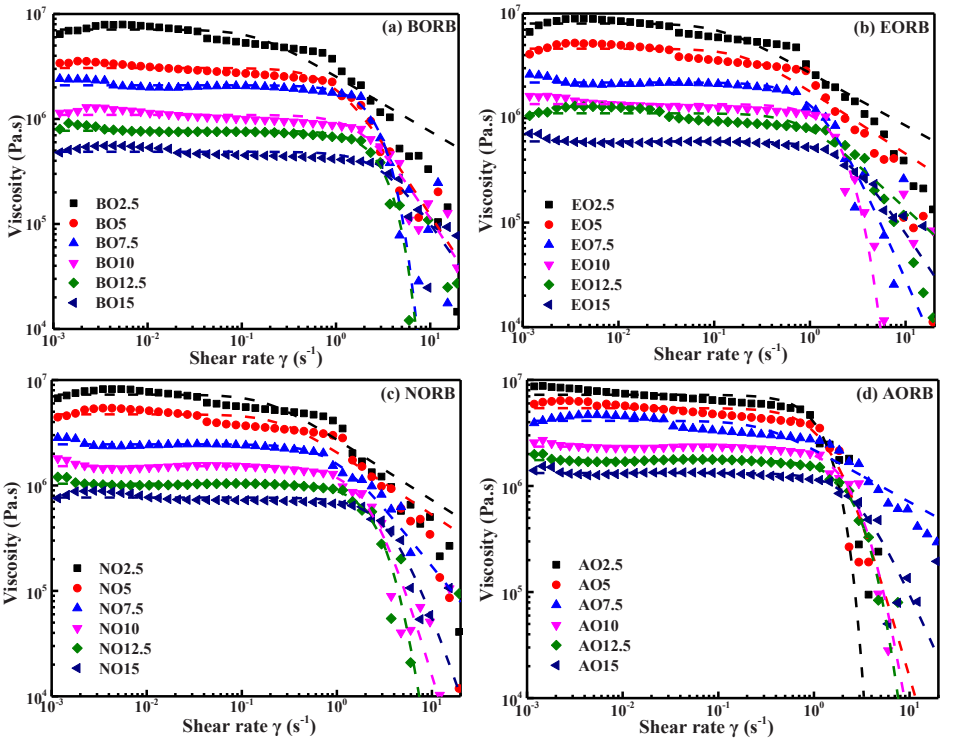

Fig. 7. Flow curves of LAB40 rejuvenated bitumen.

$$\frac{\eta_0}{\eta} = [1 + (\frac{\gamma}{\gamma_c})^2]^s \tag{10}$$

where η and γ refer to the viscosity (Pa·s) and shear rate (s^{-1}), respectively; η_0 shows the zero-shear viscosity (ZSV, Pa·s) defined as the complex viscosity value with zero external shear rate; γ_c and s are the constants. Moreover, the γ_c parameter is related to the shear rate of the shear-thinning occurring, and the s index reflects the reduction slope of the viscosity in the Non-Newtonian fluid stage [44,45].

The Carreau model fitting curves are also shown in Fig. 6(a), and the ZSV values of fresh and aged bitumen are presented in Fig. 6(b) at different temperatures of 40 ℃, 60 ℃, and 80 ℃. The Log(ZSV) value of bitumen has a linear relationship with the long-term aging time. The increased aging level results in a higher ZSV value of bitumen, which tends to decrease as the temperature rises. The reason is that long-term aging enhances the intermolecular interactions between bitumen molecules with larger ZSV parameters and shear resistance capacity. The ZSV values of age bitumen with other aging levels can be predicted using the Log(ZSV)-t correlation formulas listed in Fig. 6(b).

Fig. 7 demonstrates different rejuvenated bitumen flow curves with variable rejuvenator types and dosages. Due to the softening effect, the complex viscosity of rejuvenated binder reduces significantly with more rejuvenators included. Furthermore, a higher

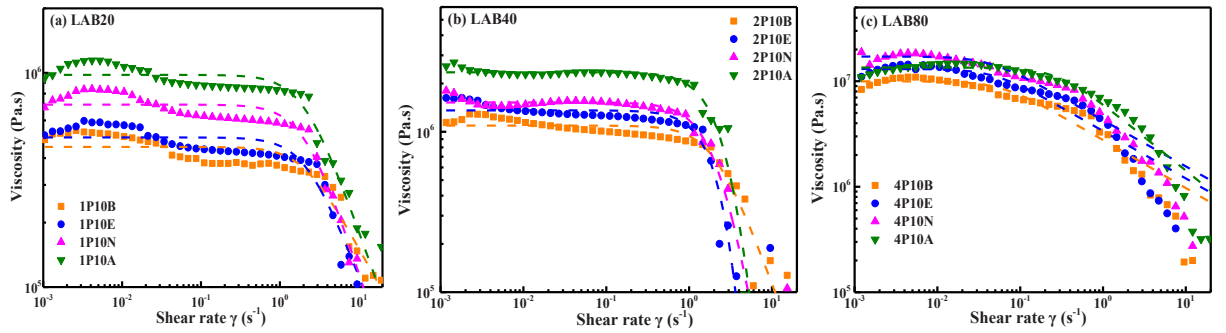

Fig. 8. Influence of aging on flow curves of rejuvenated bitumen.

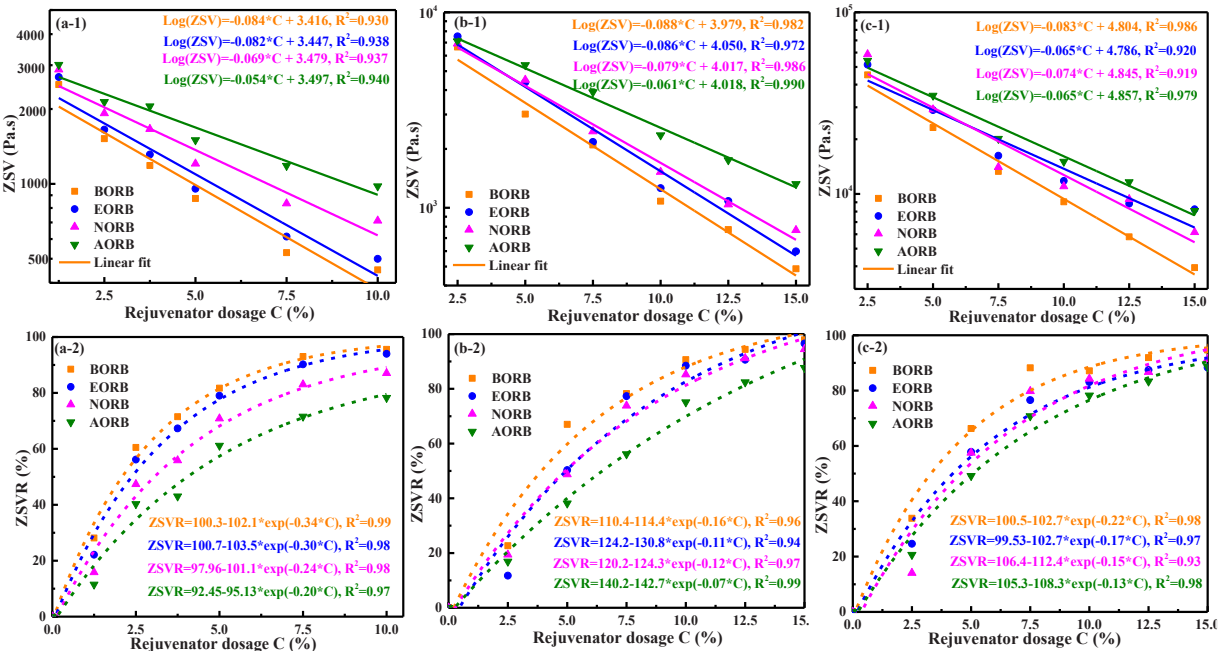

Fig. 9. Influence of rejuvenation on ZSV and ZAVR of rejuvenated bitumen (a) LAB20, (b) LAB40, and (c) LAB80.

concentration of rejuvenator expands the Newtonian-flow region within rejuvenated bitumen, exhibiting an opposite trend compared to the aging scenario. Consequently, the addition of these rejuvenators collectively serves to restore the complex viscosity levels and flow characteristics of aged bitumen towards those of fresh bitumen. Nevertheless, the rejuvenator types strongly determine the recovery situation and dosage sensitivity of viscosity. The bio-oil rejuvenator can maximally decrease the viscosity and expand the Newtonian-flow range, followed by the engine-oil and naphthenic-oil, while the AORB binder exhibits the largest viscosity and lowest sensitivity to rejuvenator content. In terms of shear resistance capability, both aromatic-oil and naphthenic-oil rejuvenators outperform bio-oil and engine-oil rejuvenators, mirroring the trend observed in the rutting parameter results. The aging effect on the flow characteristics of rejuvenated binders is displayed in Fig. 8. The intensive aging degree contributes to the enlarged viscosity of rejuvenated bitumen dramatically. The zero-shear viscosity magnitude of rejuvenated binders (AORB > NORB > EORB > AORB) is independent of the aging level of bitumen. However, the difference in complex viscosity of different rejuvenated bitumen lessens as the aging degree of bitumen deepens from LAB20 to LAB40 and LAB80.

The ZSV parameter and corresponding rejuvenation percentage ZSVR value of rejuvenated bitumen are plotted in Fig. 9. The Log (ZSV) values show a linearly decreasing trend as the rejuvenator dosage increases, regardless of rejuvenator type and aging level of bitumen. The AORB binder exhibits the highest ZSV value, whereas the BORB shows the lowest point. This suggests that an excessive use of bio-oil rejuvenator could lead to inadequate shear resistance in rejuvenated bitumen at elevated temperatures. Moreover, the ZSVR parameter increases exponentially as a function of rejuvenator content. When more rejuvenators are added, the recovery percentage on ZSV of aged bitumen presents a convergence close to 100%. Hence, it becomes challenging to distinctly discern the rejuvenating impact of these rejuvenators on the Zero-Shear Viscosity (ZSV) value of aged binder when higher rejuvenator dosages are

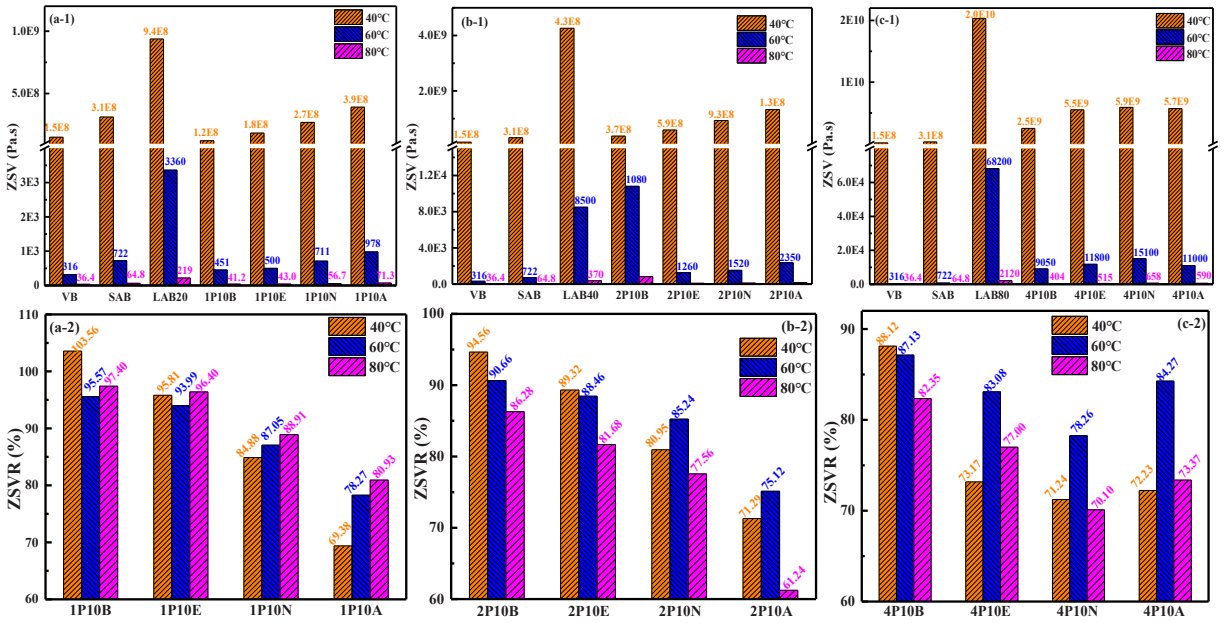

Fig. 10. Influence of temperature on ZSV and ZSVR of rejuvenated bitumen (a) LAB20, (b) LAB40, and (c) LAB80.

Table 4
The Carreau model's parameters of the virgin, aged, and rejuvenated binders.

Samples	γ_c	s	Samples	γ_c	s	Samples	γ_c	s
VB	8.71	0.65	LAB20	1.01	0.59	LAB80	0.65	1.90
SAB	2.86	0.50	LAB40	0.83	0.89	-	-	-
1P1.25B	1.58	0.93	2P2.5B	0.75	0.70	4P2.5B	0.03	0.22
1P2.5B	1.95	0.79	2P5B	1.55	0.67	4P5B	0.18	0.42
1P3.75B	2.05	0.68	2P7.5B	1.87	0.52	4P7.5B	0.36	0.52
1P5B	2.24	0.57	2P10B	1.92	0.48	4P10B	0.38	0.53
1P7.5B	2.38	0.48	2P12.5B	2.08	0.33	4P12.5B	0.45	0.53
1P10B	2.57	0.34	2P15B	2.20	0.27	4P15B	0.47	0.52
1P1.25E	1.37	0.78	2P2.5E	0.71	0.54	4P2.5E	0.02	0.22
1P2.5E	1.42	0.71	2P5E	0.89	0.80	4P5E	0.15	0.49
1P3.75E	1.75	0.65	2P7.5E	1.36	1.29	4P7.5E	0.21	0.45
1P5E	2.22	0.60	2P10E	1.42	1.04	4P10E	0.27	0.47
1P7.5E	2.27	0.55	2P12.5E	1.90	1.02	4P12.5E	0.31	0.42
1P10E	2.98	0.49	2P15E	2.09	0.70	4P15E	0.37	0.58
1P 1.25 N	1.12	0.70	2P 2.5 N	0.49	0.68	4P 2.5 N	0.01	0.38
1P 2.5 N	1.18	0.59	2P5N	0.74	0.69	4P5N	0.12	0.38
1P 3.75 N	1.20	0.58	2P 7.5 N	0.93	0.56	4P 7.5 N	0.20	0.48
1P5N	1.52	0.55	2P10N	1.39	1.57	4P10N	0.18	0.45
1P 7.5 N	2.14	0.53	2P 12.5 N	1.73	0.97	4P 12.5 N	0.23	0.45
1P10N	2.59	0.48	2P15N	2.02	1.33	4P15N	0.34	0.51
1P1.25 A	1.23	0.81	2P2.5 A	0.42	0.95	4P2.5 A	0.02	0.22
1P2.5 A	1.42	0.62	2P5A	0.67	0.94	4P5A	0.03	0.48
1P3.75 A	1.58	0.57	2P7.5 A	1.03	0.55	4P7.5 A	0.05	0.34
1P5A	1.64	0.52	2P10A	1.21	1.02	4P10A	0.08	0.46
1P7.5 A	1.96	0.53	2P12.5 A	1.67	1.04	4P12.5A	0.12	0.35
1P10A	2.07	0.53	2P15A	2.05	1.02	4P15A	0.16	0.56

employed. The difference in ZSVR values of BORB and AORB binders is significant, but EORB and NORB show similar ZSVR parameters, especially when the aged bitumen is LAB40 or LAB80. In contrast to G* /sinδ, the ZSV parameter has limitations when it comes to distinguishing the rejuvenation effectiveness of engine-oil and naphthenic-oil rejuvenators in highly aged bitumen.

The ZSV values of rejuvenated binders are measured at different temperatures to detect the temperature effect on the ZSV-based rejuvenation efficiency of various rejuvenator-aged bitumen blends. The ZSV and ZSVR results are displayed in Fig. 10. As anticipated, elevated testing temperatures result in a noteworthy decrease in the ZSV values of rejuvenated bitumen. Furthermore, the ZSVR parameters of rejuvenated bitumen vary at different temperatures. However, reaching a unified conclusion is challenging, as the temperature sensitivity of the ZSVR value also hinges on the type of rejuvenator used. Regardless of temperatures, and ZSVR order of

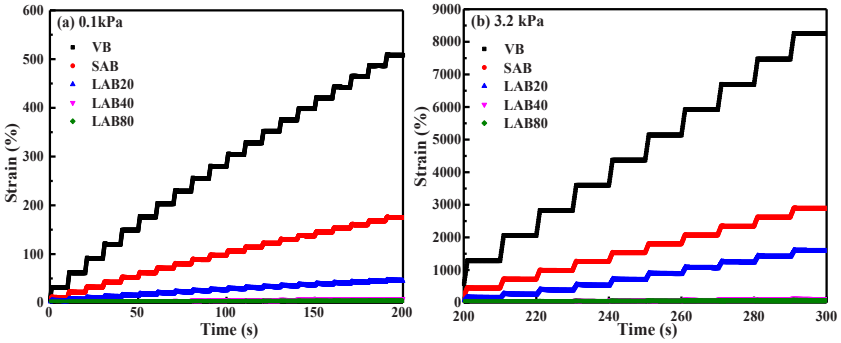

Fig. 11. The MSCR curves of fresh and aged bitumen.

rejuvenated binders at LAB20 and LAB40 is the same as BORB > EORB > NORB > AORB. Therefore, the bio-oil rejuvenator would weaken the shear-resistance performance of aged bitumen to the greatest extent, while the aromatic-oil shows the largest retention effect.

Moreover, the degree of bitumen aging influences the pattern of change in ZSVR values concerning temperature and the type of rejuvenator. These ZSVR values progressively decrease as the aging level intensifies. When the bitumen is severely aged (LAB80), the ZSVR values at 60 ℃ of 4P10E, 4P10N, and 4P10A are higher than that at 40 ℃ and 80 ℃. Due to the elevated stiffness of LAB80, the rejuvenation impact of rejuvenators (EO, NO, AO) on the ZSV parameter is constrained at lower temperatures. However, bio-oil, possessing greater molecular mobility, can still effectively restore the ZSV. Interestingly, the ZSVR value for 4P10A surpasses that of 4P10N, indicating that the rejuvenating effect of aromatic-oil on the flow characteristics of severely aged bitumen becomes more pronounced. This phenomenon can be attributed to the strong polarity of aromatic-oil, which robustly interacts with and dissolves asphaltene clusters, thereby expediting the reconstruction of the colloidal structure in aged bitumen [46].

Table 4 lists the γ_c and s parameters in Carreau models of fresh, aged, and rejuvenated binders. The γ_c decreases and the s parameter increases distinctly during the long-term aging process. This indicates that increased aging levels reduce the extent of the Newtonian-fluid region and amplify the susceptibility of complex viscosity to shear rate changes. The introduction of rejuvenators enhances the γc value while reducing the s parameter of aged bitumen to levels comparable to fresh bitumen. This implies that these four rejuvenators have the capacity to rejuvenate the flow properties of aged bitumen, with their effectiveness being notably impacted by the type of rejuvenator, dosage, and the degree of bitumen aging. In detail, the rejuvenator content shows a positive connection with the γ_c parameter but a negative relationship with the s value of rejuvenated bitumen. Moreover, a high aging degree of bitumen results in a lower γ_c and a higher s value. It should be mentioned that the ZSV parameter directly related to the high-temperature shear resistance of bitumen will be analyzed as the potential indicator for rejuvenation efficiency evaluation. While it is observed that aging and rejuvenation conditions have notable effects on flow characteristics such as the γ_c and s parameters, establishing a direct link between these parameters and high-temperature mechanical performance poses a challenge. Consequently, this study does not delve into the discussion of these flow parameters, as they will be subject to further exploration in future research.

4.3. Anti-deformation capacity from MSCR test

4.3.1. MSCR curves of fresh, aged, and rejuvenated bitumen

The MSCR test always characterizes the high-temperature deformation and recovery capacity of bituminous material [47]. Fig. 11 illustrates the MSCR curves of fresh and aged bitumen at two stress levels of 0.1 and 3.2 kPa. The increased applied stress and loading time both enlarge the strain of bitumen. With an escalation in aging level, the strain value gradually decreases owing to the heightened stiffness of aged bitumen. This observation indicates that a higher degree of aging enhances the deformation resistance of bitumen, a trend that aligns with findings in both the LVE rutting parameter and flow characteristics. Different parameters are outputted from MSCR curves to quantitatively evaluate the effects of aging and rejuvenation on the deformation potential and elastic performance of bitumen, including the recovery percentage ($R_{0.1}$, $R_{3.2}$), non-recoverable creep compliance ($J_{nr0.1}$, $J_{nr3.2}$), and stress sensitivity parameters (R_{diff}, J_{nrdiff}).

Fig. 12 displays the MSCR parameters of fresh and aged bitumen. The $R_{0.1}$ and $R_{3.2}$ values of bitumen tend to increase exponentially as the aging degree deepens. Meanwhile, the aging time extension leads to an exponential reduction of parameters $J_{nr0.1}$, $J_{nr3.2}$, R_{diff}, and J_{nrdiff}. Additionally, the temperature greatly influences bitumen's elastic recovery and creep potential. As the temperature rises, the R-value decreases while Jnr, R_{diff}, and J_{nrdiff} enlarge. It means that high temperatures weaken the elastic recovery and increase the deformation level and stress sensitivity of bitumen. As the stress level increases from 0.1 kPa to 3.2 kPa, the R-value decreases, and J_{nr} increases. Therefore, the aging impact on the MSCR parameters of bitumen depends on the temperature and stress level, which should be considered in the following rejuvenation process. Further, these MSCR parameters of aged bitumen with other aging levels can be predicted by the listed correlation equations between the MSCR parameters and aging time.

The MSCR curves of LAB40 rejuvenated bitumen with variable rejuvenator type and dosage are shown in Fig. 13. Regardless of rejuvenator type and stress level, the increment in rejuvenator content enlarges the strain value of rejuvenated bitumen. This can be

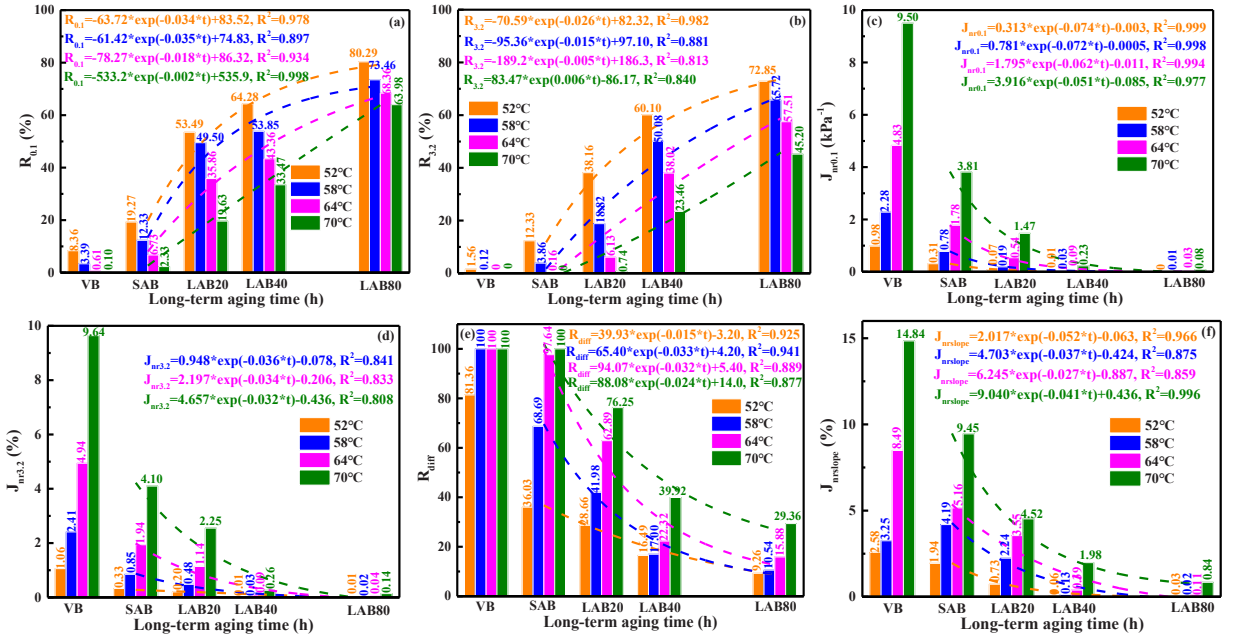

Fig. 12. Influence of aging on the MSCR indices of bitumen.

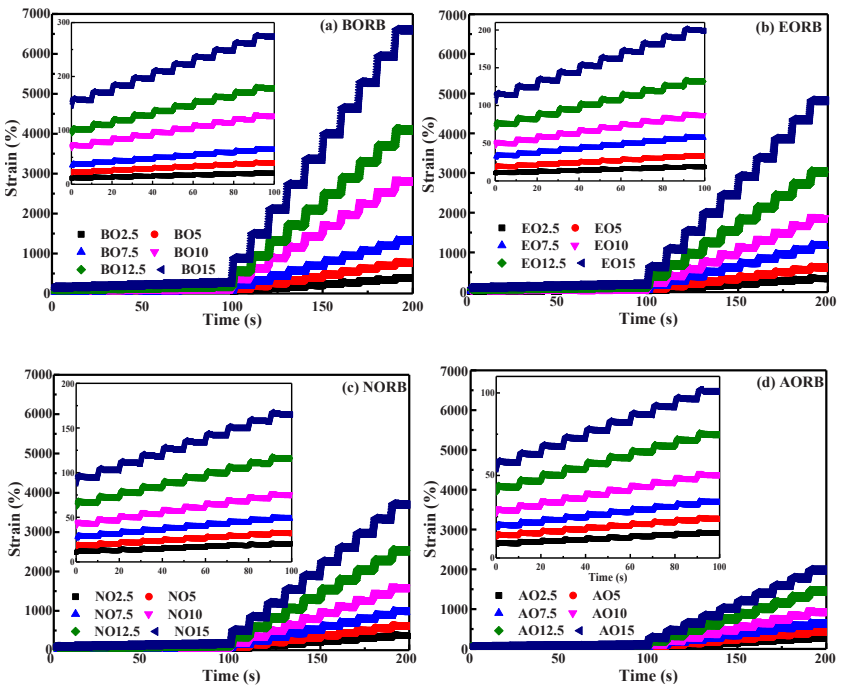

Fig. 13. The MSCR curves of LAB40 rejuvenated bitumen.

ascribed to the softening impact of rejuvenators, as their inclusion diminishes the deformation resistance of aged bitumen. Additionally, different rejuvenators exert distinct effects on the elastic recovery and creep properties of aged bitumen. When the stress level, loading time, and rejuvenator dosage keep constant, the ranking of strain value of rejuvenated bitumen is BORB > EORB > NORB > AORB. Thus, the bio-oil rejuvenator shows the largest effect on softening the aged bitumen, and the aromatic-oil rejuvenated bitumen exhibits the strongest deformation resistance. Additionally, the stress level significantly impacts the MSCR curves of rejuvenated bitumen more than the rejuvenator type and dosage.

The effect of the aging level on the MSCR curves of rejuvenated bitumen is reflected in Fig. 14. As expected, the increased aging

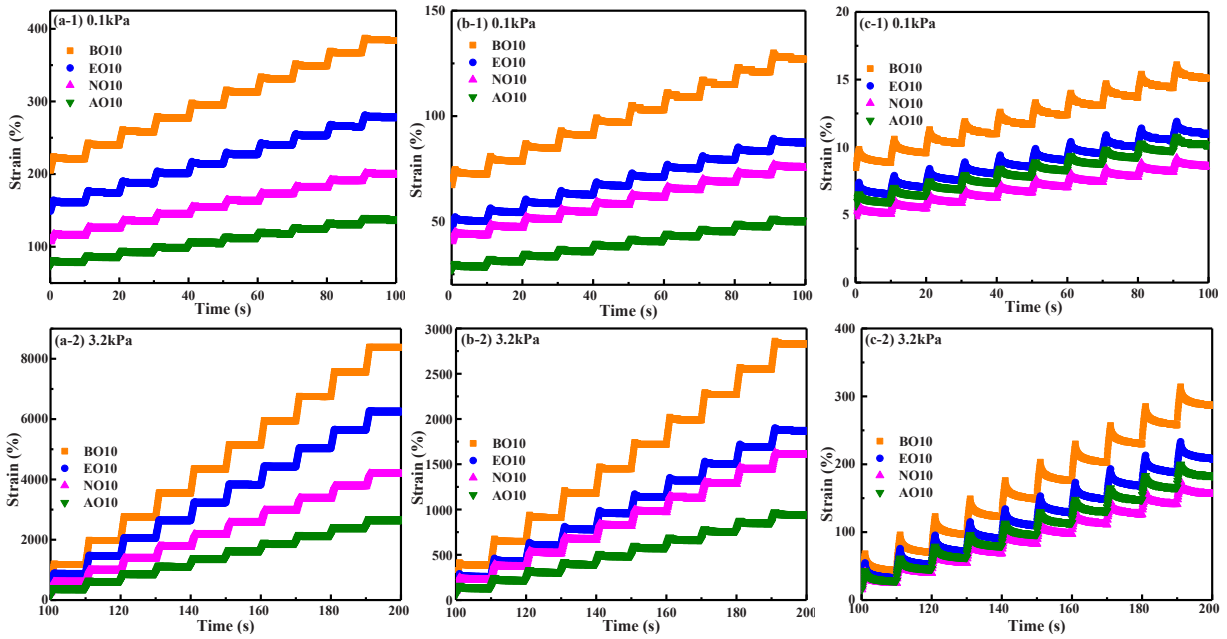

Fig. 14. Aging effect on the MSCR curves of rejuvenated bitumen, (a-1)(a-2) LAB20, (b-1)(b-2) LAB40, and (c-1)(c-2) LAB80.

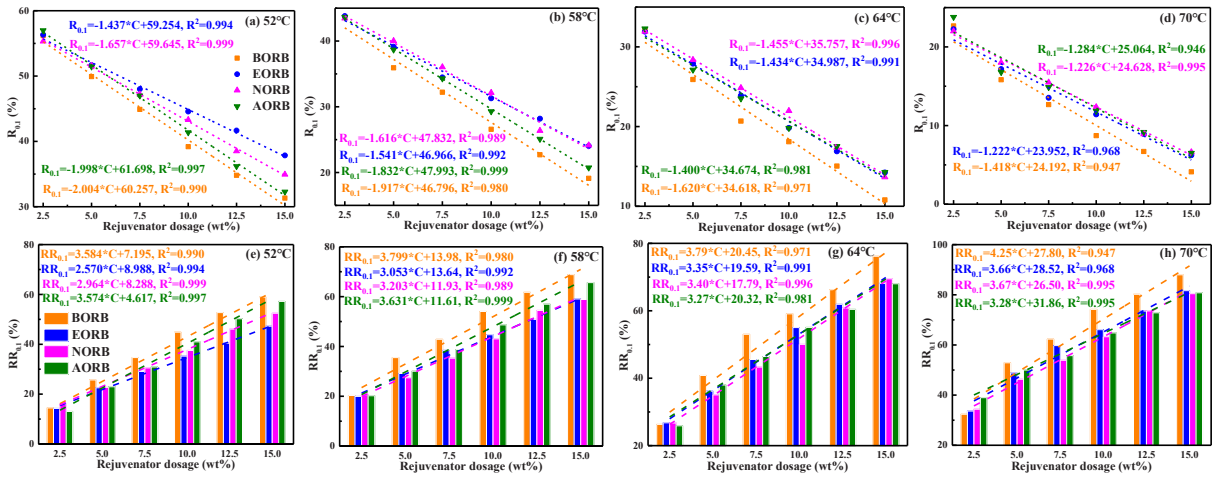

Fig. 15. The influence of rejuvenator dosage on the $R_{0.1}$ and $RR_{0.1}$ value.

level declines the strain value, indicating that the high aging degree positively affects the anti-deformation performance of rejuvenated bitumen. The aging influence is more obvious at a higher stress level. In addition, the aging degree has less effect on the strain order of rejuvenated binders (BO > EO > NO > AO), but the ranking becomes less significant as the aging level of bitumen deepens. Interestingly, the strain values of AO10 are lower than NO10 when the aging bitumen is LAB80. The strong intermolecular interaction and compatibility between the aromatic-oil and severely-aged bitumen molecules would accelerate the deagglomeration of asphaltene clusters.

4.3.2. $R_{0.1}$ parameter of rejuvenated bitumen

The $R_{0.1}$ parameter and corresponding rejuvenation percentage $RR_{0.1}$ of rejuvenated bitumen are plotted in Fig. 15 at different temperatures of 52, 58, 64, and 70 ℃. Regardless of rejuvenator type and temperature, the $R_{0.1}$ value of rejuvenated bitumen decreases linearly as a function of rejuvenator dosage, and the $RR_{0.1}$ value enlarges linearly. At all temperatures, the $R_{0.1}$ and $RR_{0.1}$ value of the BORB binder is the minimum and maximum. It indicates that bio-oil rejuvenator maximally weakens the elastic recovery capacity of aged bitumen. Interestingly, the $R_{0.1}$ of AORB is lower than EORB and NORB due to the low-stress level. This result does not agree with the LVE G* /sinδ and flow ZSV conclusion (BORB < EORB < NORB < AORB). Thus, the $R_{0.1}$ parameter is inappropriate for assessing

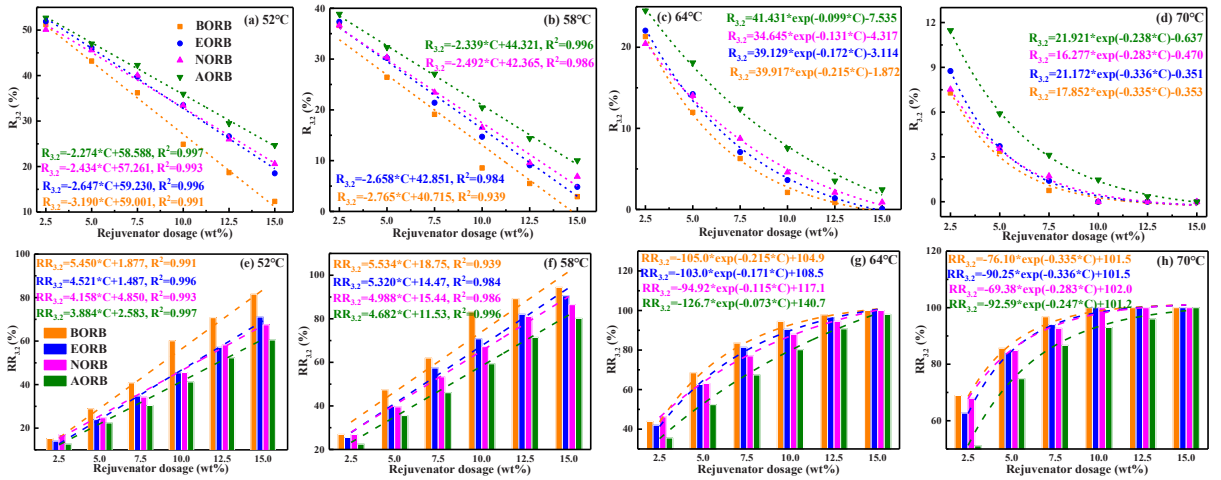

Fig. 16. The influence of rejuvenator dosage on the $R_{3.2}$ values of rejuvenated bitumen.

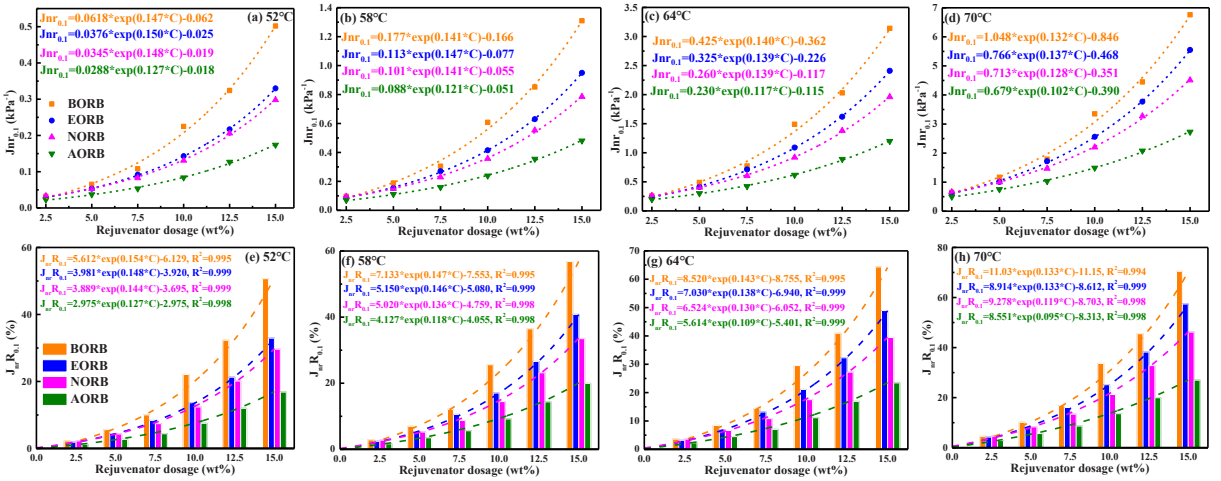

Fig. 17. The influence of rejuvenator dosage on the $Jnr_{0.1}$ value of rejuvenated bitumen.

and distinguishing the various rejuvenators' effects on the high-temperature performance of aged binders.

4.3.3. *$R_{3.2}$ parameter of rejuvenated bitumen*

Fig. 16 illustrates the $R_{3.2}$ and $RR_{3.2}$ values of rejuvenated binders. With the increase in rejuvenator dosage, the $R_{3.2}$ parameter decreases linearly or exponentially, depending on the temperature, while the $RR_{3.2}$ tends to increase relatively. It should be noticed that the $R_{3.2}$ ($RR_{3.2}$) values of various rejuvenated bitumen can be differentiated as a ranking of BORB < EORB < NORB < AORB (converse for $RR_{3.2}$), which is the same as the LVE rutting parameter and flow results. Therefore, the $R_{3.2}$ parameter can effectively evaluate the elastic recovery performance of rejuvenated binders at high temperatures. Nevertheless, the temperature affects the variation trend of $RR_{3.2}$ values of rejuvenated binders. At low temperatures (52 ℃ and 58 ℃), the $RR_{3.2}$ has a linear relationship with rejuvenator dosage, which increases exponentially at high temperatures (64 ℃ and 70 ℃). The temperature has to be mentioned when the rejuvenation effect of various rejuvenators on the elastic recovery property of aged bitumen is investigated.

4.3.4. *$J_{nr0.1}$ parameter of rejuvenated bitumen*

The variations of creep compliance $J_{nr0.1}$ and rejuvenation efficiency $J_{nr}R_{0.1}$ of rejuvenated binders versus rejuvenator dosage are shown in Fig. 17. As the rejuvenator content rises, the $J_{nr0.1}$ and $J_{nr}R_{0.1}$ values of all rejuvenated binders show an exponentially increasing trend. Regardless of temperature and rejuvenator content, the ranking of $J_{nr0.1}$ and $J_{nr}R_{0.1}$ value of rejuvenated binders is BORB > EORB > NORB > AORB. This indicates that bio-oil rejuvenated bitumen exhibits the highest creep potential, whereas aromatic-oil rejuvenated bitumen demonstrates the lowest degree of creep. Elevated temperatures expedite the increase in the JnrR0.1 value of rejuvenated bitumen, which is attributed to heightened molecular mobility. Overall, the $J_{nr0.1}$ parameter can effectively evaluate and distinguish the effects of these rejuvenators on the high-temperature creep potential of aged bitumen, but the

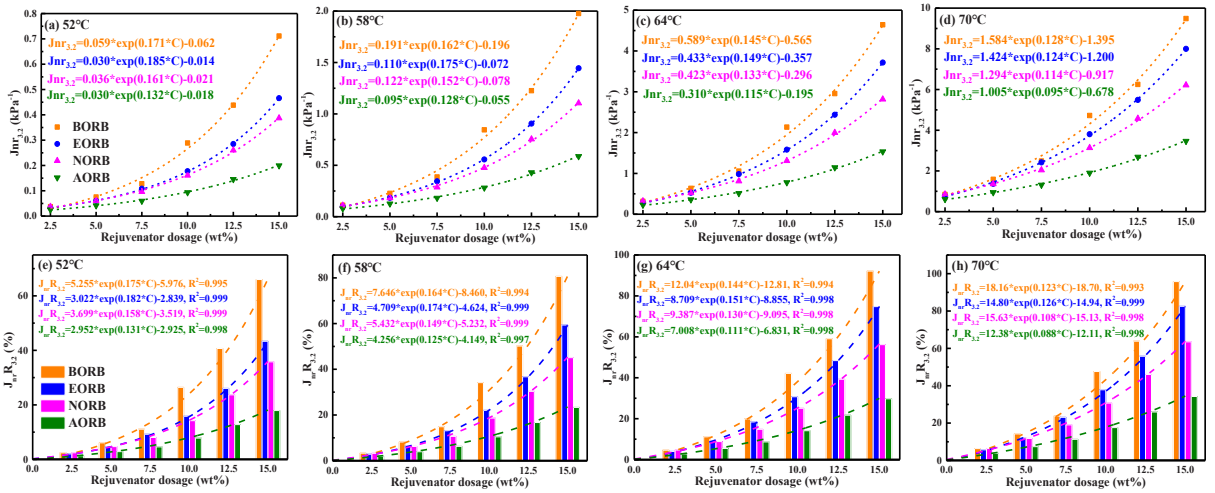

Fig. 18. The influence of rejuvenator dosage on the $Jnr_{3.2}$ value of rejuvenated bitumen.

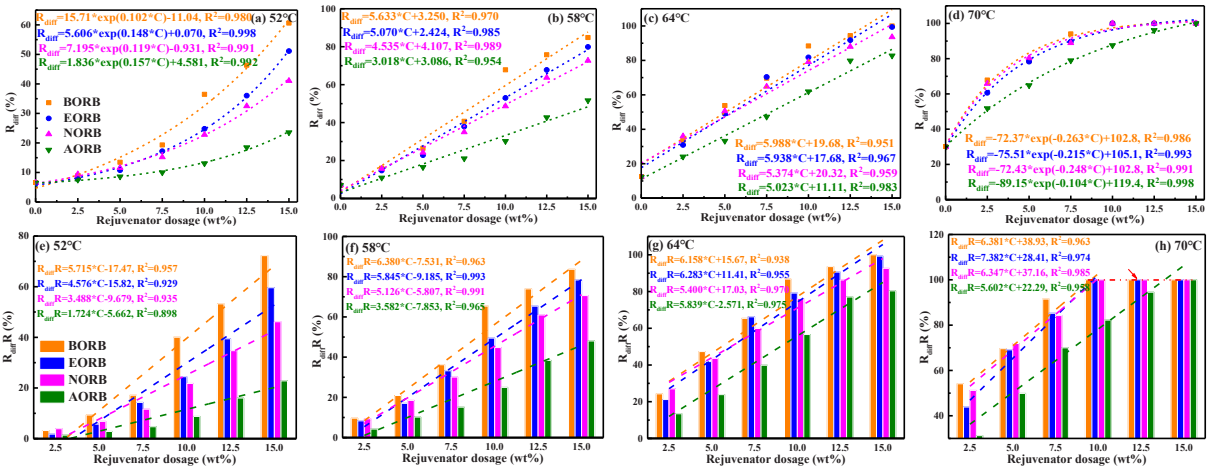

Fig. 19. The influence of rejuvenator dosage on the R_{diff} value of rejuvenated bitumen.

rejuvenation efficiency based on the $J_{nr0.1}$ parameter is dependent on temperature.

4.3.5. *$J_{nr3.2}$ parameter of rejuvenated bitumen*

Fig. 18 shows $J_{nr3.2}$ and $J_{nr}R_{3.2}$ curves versus rejuvenator dosages of different rejuvenated bitumen. Similar to the $J_{nr0.1}$ index, the $J_{nr3.2}$ and $J_{nr}R_{3.2}$ values of rejuvenated binders increase exponentially as rejuvenator content increases. Meanwhile, the ranking of $J_{nr3.2}$ and $J_{nr}R_{3.2}$ is BORB > EORB > NORB > AORB, the same as $J_{nr0.1}$ and $J_{nr}R_{0.1}$. Therefore, both $J_{nr0.1}$ and $J_{nr3.2}$ can be effective indicators for assessing the rejuvenation effects of various rejuvenators on the high-temperature creep performance of aged bitumen. Compared to $J_{nr}R_{0.1}$, the $J_{nr}R_{3.2}$ values are slightly higher when the rejuvenator type/dosage and aging degree of bitumen is the same. Measuring the $J_{nr0.1}$ and $J_{nr3.2}$ parameters of rejuvenated bitumen is unnecessary, but the stress level and temperature should keep constant when comparing the rejuvenation efficiency of different rejuvenators.

4.3.6. *R_{diff} parameter of rejuvenated bitumen*

The stress sensitivity of rejuvenated binders is estimated with parameters R_{diff} and $J_{nrslope}$. Fig. 19 shows the influence of rejuvenator type/dosage and temperature on aged bitumen's R_{diff} and $R_{diff}R$ values. As the rejuvenator content increases, the R_{diff} values enlarge gradually, but the variation trend depends on the temperature. This illustrates that the stress sensitivity of rejuvenated bitumen becomes more pronounced with increasing rejuvenator content. Irrespective of the rejuvenator dosage and temperature, bio-oil rejuvenated bitumen exhibits the highest $R_{diff,}$ followed by engine-oil and naphthenic-oil rejuvenated binders, while aromatic-oil rejuvenated bitumen displays the lowest R_{diff}. In addition, the order of $R_{diff}R$ values of rejuvenated binders is BORB > EORB > NORB > AORB. Nevertheless, the temperature significantly affects the $R_{diff}R$ values of rejuvenated binders. When the temperature is 70 ℃, and the rejuvenator dosage exceeds 10%, the $R_{diff}R$ values of BORB, EORB, and NORB binders converse to 100%. Therefore, the

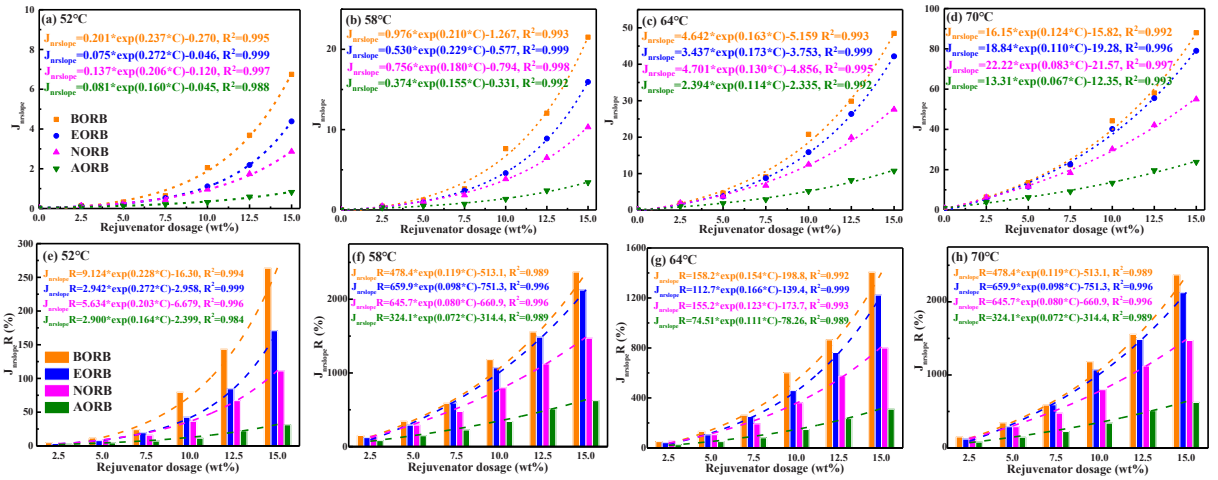

Fig. 20. The influence of rejuvenator dosage on the Jnr_{slope} value at different temperatures.

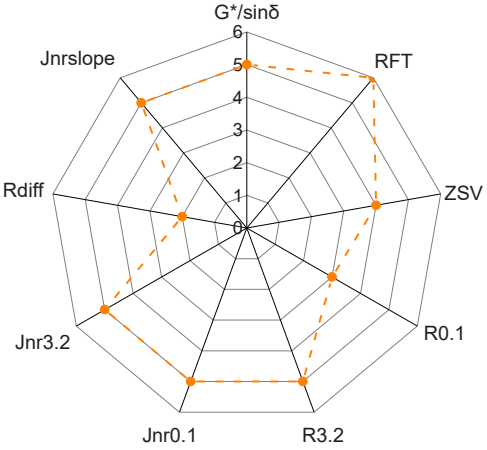

Fig. 21. Score for critical high-temperature indicators.

temperature should be lower than 64 ℃ to effectively assess the influence of rejuvenator content on the $R_{diff}R$ value and differentiate the rejuvenation efficiency of various rejuvenators.

4.3.7. $J_{nrslope}$ parameter of rejuvenated bitumen

Fig. 20 illustrates the $J_{nrslope}$ and $J_{nrslope}R$ parameters of rejuvenated binders. As rejuvenator content increases, the $J_{nrslope}$ and $J_{nrslope}R$ values enlarge exponentially. Moreover, high temperature promotes the enhancement in both $J_{nrslope}$ and $J_{nrslope}R$ values. When the temperature and rejuvenator content keep constant, the ranking of $J_{nrslope}$ and $J_{nrslope}R$ of rejuvenated binders is the same as R_{diff} (BORB > EORB > NORB > AORB). Compared to the R_{diff} parameter, there is no convergence point in $J_{nrslope}$-C and $J_{nrslope}R$-C curves. Additionally, the difference in $J_{nrslope}R$ values of different rejuvenated binders is significant. Thus, the $J_{nrslope}$ parameter can be an effective indicator for evaluating the rejuvenation efficiency of various rejuvenators on the stress sensitivity of aged bitumen.

4.4. Critical indicators recommendation and their potential connections

It is detected that the rejuvenation efficiency of rejuvenators on high-temperature elastic and recovery performance of aged bitumen depends on the evaluation methods and indicators. In this section, the sensitivity levels of different indicators from the LVE rutting, flow, and MSCR tests are calculated and compared in Fig. 21. It should be mentioned that the score of these critical high-temperature indicators contains six terms: rejuvenation potential; sensitivity to rejuvenator dosage and type; sensitivity to aging degree of bitumen; temperature influence; and the scope of rejuvenation percentages. It is more possible for a high-temperature indicator with a higher score to effectively evaluate and distinguish the rejuvenation effects of various rejuvenator-aged bitumen blends.

As shown in Fig. 21, the G* /sinδ and RFT parameters from the LVE test show score of 5 and 6, while the ZSV index only presents a score of 4. Regarding the MSCR parameters, the $R_{3.2}$, $J_{nr0.1}$, $J_{nr3.2}$, and $J_{nrslope}$ score the same 5, but $R_{0.1}$ and R_{diff} have low scores of 3

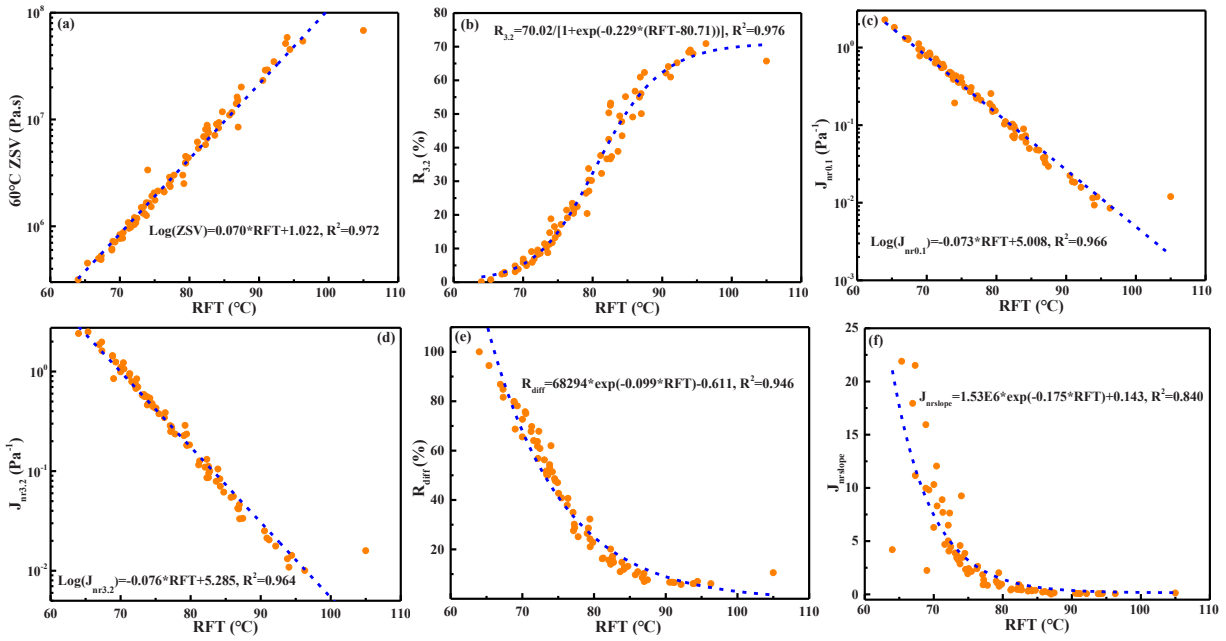

Fig. 22. Correlations between the RFT with other critical evaluation indicators.

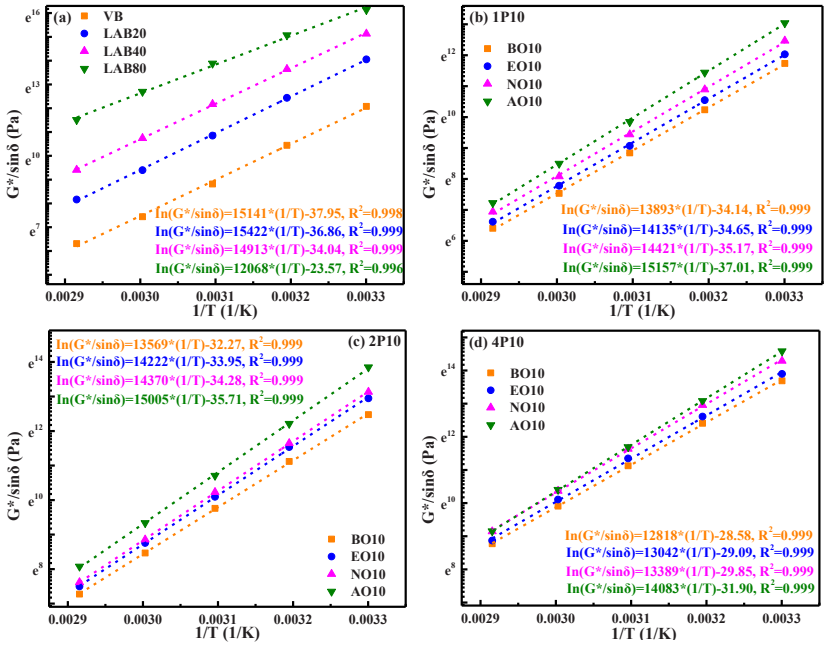

Fig. 23. Log(G*/sinδ)− 1/T correlation curves of rejuvenated bitumen.

and 2, respectively. Based on the score result, the parameters RFT and ZSV can be effective indicators from LVE and flow test, whereas $R_{3.2}$, $J_{nr0.1}$or $J_{nr3.2}$, and $J_{nrslope}$ parameters are recommended to estimate the elastic performance, creep potential, and stress sensitivity of rejuvenated bitumen.

In addition, the RFT index exhibits the highest score than ZSV and MSCR parameters, indicating that the RFT parameter is the first choice to evaluate and differentiate the high-temperature performance of various rejuvenator-aged bitumen systems. However, the flow and MSCR tests reflect the deformation capacity of bituminous materials. Therefore, it is important to correlate the RFT index with other parameters, which are plotted in Fig. 22. It is observed that the RFT index correlates well with other effective high-temperature indicators. Regardless of rejuvenation conditions (rejuvenator type/dosage and aging degree of bitumen), the RFT

Table 5
Ea and A parameters of rejuvenated binders.

Samples	Ea	A	Samples	Ea	A	Samples	Ea	A
VB	125882	3.3E-17	LAB20	128219	9.8E-17	LAB80	100333	5.8E-11
SAB	127129	5.2E-17	LAB40	123987	1.6E-15			
1P1.25B	124461	3.2E-16	2P2.5B	118599	5.3E-15	4P2.5B	107009	1.2E-12
1P2.5B	122515	4.2E-16	2P5B	117128	5.4E-15	4P5B	109121	3.6E-13
1P3.75B	121592	4.6E-16	2P7.5B	116471	4.7E-15	4P7.5B	107890	1.3E-13
1P5B	121243	4.1E-16	2P10B	112813	9.7E-15	4P10B	106569	3.9E-13
1P7.5B	118674	6.8E-16	2P12.5B	110194	1.9E-14	4P12.5B	104008	6.5E-13
1P10B	115506	1.5E-15	2P15B	113087	4.6E-14	4P15B	103717	5.2E-13
1P1.25E	126107	1.9E-16	2P2.5E	120894	2.5E-15	4P2.5E	109155	5.4E-13
1P2.5E	123895	2.6E-16	2P5E	118233	4.1E-15	4P5E	111408	1.7E-13
1P3.75E	123787	2.5E-16	2P7.5E	119913	1.4E-15	4P7.5E	106694	5.2E-13
1P5E	121767	3.6E-16	2P10E	118242	1.8E-15	4P10E	108431	2.3E-13
1P7.5E	122207	2.2E-16	2P12.5E	118341	1.2E-15	4P12.5E	108847	1.5E-13
1P10E	117518	9.0E-16	2P15E	118292	9.0E-16	4P15E	108082	1.7E-13
1P 1.25 N	125084	2.8E-16	2P 2.5 N	121734	1.7E-15	4P 2.5 N	107783	1.1E-12
1P 2.5 N	124818	2.3E-16	2P5N	120237	2.0E-15	4P5N	111275	2.2E-13
1P 3.75 N	124643	2.1E-16	2P 7.5 N	119796	1.7E-15	4P 7.5 N	108423	3.3E-13
1P5N	123330	3.5E-16	2P10N	119472	1.3E-15	4P10N	111316	1.1E-13
1P 7.5 N	123056	2.1E-16	2P 12.5 N	118150	1.5E-15	4P 12.5 N	108331	2.4E-13
1P10N	119896	5.3E-16	2P15N	117477	1.4E-15	4P15N	110560	8.2E-14
1P1.25 A	125575	2.5E-16	2P2.5 A	124037	10E-16	4P2.5 A	112863	1.7E-13
1P2.5 A	128684	6.3E-17	2P5A	124369	6.4E-16	4P5A	115698	4.3E-14
1P3.75 A	128293	6.7E-17	2P7.5 A	124186	5.2E-16	4P7.5 A	115240	2.9E-14
1P5A	128950	4.2E-17	2P10A	124752	3.1E-16	4P10A	117086	1.4E-14
1P7.5 A	127653	5.4E-17	2P12.5 A	125882	1.5E-16	4P12.5A	118375	6.5E-15
1P10A	126015	8.5E-17	2P15A	126248	1.1E-16	4P15A	121251	1.8E-15

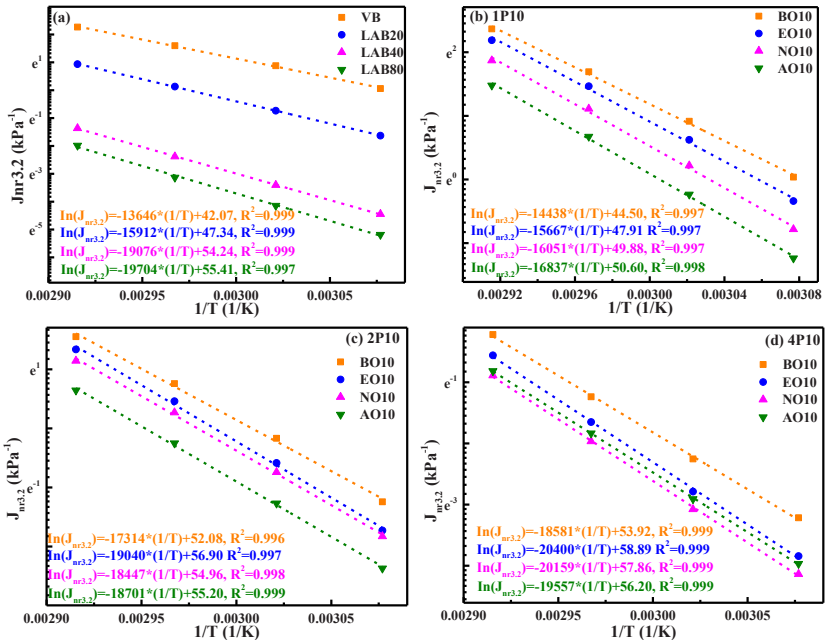

Fig. 24. Log($J_{nr3.2}$)– 1/T correlation curves of rejuvenated bitumen.

parameter shows a positive linear relationship with the ZSV index but has a negative linear correlation with the $J_{nr0.1}$ and $J_{nr3.2}$. Moreover, the $R_{3.2}$ value of rejuvenated bitumen tends to increase exponentially as a function of the RFT parameter. In addition, the stress sensitivity parameters, R_{diff} and $J_{nrslope}$, decrease exponentially as the RFT value rises. Therefore, the RFT index from the LVE test can be measured first, and the flow and MSCR parameters will be further predicted using these correlation equations.

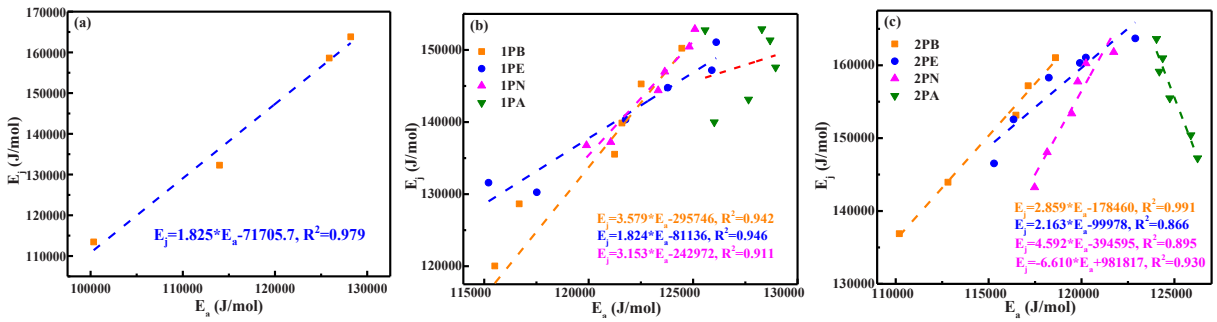

Fig. 25. Relationship between the activation energy based on LVE and MSCR tests.

4.5. *Temperature susceptibility at the high-temperature region*

The temperature susceptibility of rejuvenated binders is evaluated through the Log(G*/sinδ)-(1/T) correlation curves, shown in Fig. 23. The G* /sinδ values of fresh, aged, and rejuvenated binders enlarges linearly as the increase in 1/T. With the aging degree deepening, the slope value decreases, indicating that the temperature sensitivity weakens. Different rejuvenated bitumen exhibits the variable change trend of G* /sinδ to temperature. The slope ranking of rejuvenated bitumen is BORB < EORB < NORB < AORB, and a high aging level reduces the temperature susceptibility of rejuvenated bitumen. The activation energy Ea and precondition parameter A are calculated by the Arrhenius equation shown below:

$$\mathrm{Ln(H)} = \frac{\mathrm{Ea}}{\mathrm{R}} \bullet \frac{1}{\mathrm{T}} + \mathrm{Ln(A)} \tag{11}$$

where H refers to high-temperature parameters (G*/sinδ or $J_{nr3.2}$), Ea is the activation energy, and R is gas constant (8.314 $J{\cdot}mol^{-1}{\cdot}K^{-1}$). Table 5 lists the Ea and A values of rejuvenated bitumen. The Ea value of bitumen declines gradually as the aging degree deepens. Moreover, the Ea values of rejuvenated bitumen tend to reduce as the rejuvenator dosage rises. In addition, the rejuvenator type greatly influences the Ea and A of rejuvenated bitumen. The bio-oil rejuvenated bitumen exhibits the lowest Ea value, followed by the engine-oil and naphthenic-oil rejuvenated bitumen, and the aromatic-oil rejuvenated bitumen has the largest Ea value. It denotes that the bio-oil rejuvenator maximizes the temperature sensitivity, while the aromatic-oil rejuvenated bitumen presents the smallest temperature susceptibility.

Fig. 24 illustrates the $\mathrm{Log}(J_{nr3.2})-1/T$ curves of rejuvenated bitumen to detect the influence of high-temperature parameters on the temperature sensitivity result. As the increase of (1/T), the $\mathrm{Ln}(J_{nr3.2})$ values of fresh, aged, and rejuvenated bitumen decrease linearly. The long-term aging promotes the sensitivity of bitumen $J_{nr3.2}$ value to (1/T). Meanwhile, it is found that the rejuvenator type and aging degree of bitumen both contribute to the variation trend of $J_{nr3.2}$-1/T curves of rejuvenated binders. The Jnr3.2 value of bio-oil rejuvenated binder shows the lowest temperature sensitivity. The activation energy E_j of rejuvenated bitumen is calculated based on $J_{nr3.2}$-1/T correlations, and its relationship with the E_a parameter is shown in Fig. 25. It is demonstrated that the E_j values of fresh, aged, and rejuvenated binders exhibit linear correlations with the corresponding E_a parameter. It means that both G* /sinδ and $J_{nr3.2}$ indices show similar functions to reflect the temperature sensitivity of bituminous material. However, the E_j-E_a curves of rejuvenated binders are significantly affected by the rejuvenator type and the aging degree of bitumen. Interestingly, the E_j value of aromatic-oil rejuvenated bitumen shows a negative linear connection with the Ea parameter. Thus, the G* /sinδ and $J_{nr3.2}$ indices exhibit the opposite effect on assessing the temperature susceptibility of aromatic-oil rejuvenated bitumen.

5. Conclusions and recommendations

This study aims to systematically investigate the complex effects of rejuvenator type/dosage and aging degree of bitumen on the high-temperature performance of rejuvenated bitumen. The variations of rutting, flow, and elastic/creep parameters of rejuvenated binders are compared to propose the critical indicators for evaluating and distinguishing the rejuvenation efficiency of different rejuvenators on the high-temperature property of bitumen. The main findings are listed as follows:

(1) The bio-oil rejuvenator maximally weakens the high-temperature performance of aged bitumen, followed by the engine-oil and naphthenic -oil, while the aromatic-oil rejuvenated bitumen exhibits the best rutting, flow, and creep resistance.
(2) Based on the score result, the parameters RFT and ZSV can be effective indicators from LVE and flow test, whereas $R_{3.2}$, $J_{nr0.1}$or $J_{nr3.2}$, and $J_{nrslope}$ parameters are recommended to estimate the elastic performance, creep potential, and stress sensitivity of rejuvenated bitumen.
(3) The RFT parameter is recommended as the critical indicator for effectively evaluating and differentiating the rejuvenation effectiveness of various rejuvenators on the high-temperature performance of aged bitumen. In addition, the RFT index correlates well with other effective high-temperature indicators.

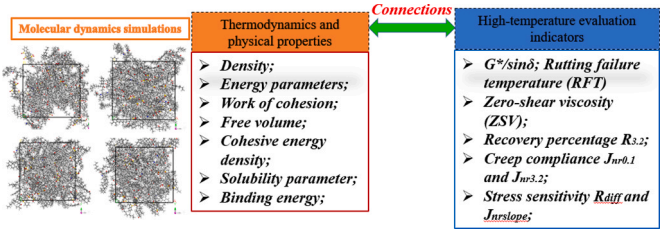

Fig. 26. Future study on connections between thermodynamics properties and high-temperature evaluation indicators of rejuvenated bitumen.

(4) The temperature sensitivity outputs of rejuvenated bitumen based on G* /sinδ and $J_{nr3.2}$ values are similar but strongly affected by the rejuvenator type. The aromatic-oil rejuvenated bitumen shows a different change trend of the E_a-E_j curve with the other three rejuvenated binders.

This paper mainly concentrates on the macroscale rheological evaluation of the high-temperature performance of different rejuvenator-aged bitumen blends. In future work, the microscale underlying mechanism on the difference in rejuvenation efficiency of various rejuvenators on high-temperature rutting, flow, elastic and creep performance of aged bitumen using multiscale evaluation methods (such as chemical characterizations, molecular dynamics simulations, and morphological observations), as shown in Fig. 26.

Declaration of Competing Interest

The authors declare that they have no known competing financial interests or personal relationships that could have appeared to influence the work reported in this paper.

Data Availability

Data will be made available on request.

References

[1] B. Li, W. Liu, X. Nan, J. Yang, C. Tu, L. Zhou, Development of rejuvenator using waste vegetable oil and its influence on pavement performance of asphalt binder under ultraviolet aging, Case Stud. Constr. Mater. 18 (2023), e01964.
[2] S. Yan, Q. Dong, X. Chen, C. Zhou, S. Dong, X. Gu, Application of waste oil in asphalt rejuvenation and modification: a comprehensive review, Constr. Build. Mater. 340 (2022), 127784.
[3] L. Wang, A. Shen, G. Mou, Y. Guo, M. Yang, Effect of RAP gradation subdivision and addition of a rejuvenator on recycled asphalt mixture engineering performance, Case Stud. Constr. Mater. 18 (2023), e02136.
[4] D. Wang, J. Zhu, L. Porot, A. Falchetto, S. Damen, Multiple stress creep and recovery test for bituminous binders-influence of several key experimental parameters, Road. Mater. Pavement Des. (2023) 2180992.
[5] F. Santos, A. Faxina, S. Soares. Soy-based rejuvenated asphalt binders: impact on rheological properties and chemical aging indices, Constr. Build. Mater. 300 (2021), 124220.
[6] J. Yi, Y. Wang, Z. Pei, M. Xu, D. Feng, Mechanisms and research progress on biological rejuvenators for regenerating aged asphalt: review and discussion, J. Clean. Prod. (2023), 138622.
[7] K. Shi, Z. Fu, F. Ma, J. Liu, R. Song, J. Li, J. Dai, C. Li, Y. Wen, Development on the rheological properties and micromorphology of active reagent-rejuvenated SBS-modified asphalt, ACS Sustain. Chem. Eng. 10 (2022) 16734–16751.
[8] J. Wang, S. Lv, J. Liu, X. Peng, W. Lu, Z. Wang, N. Xie, Performance evaluation of aged asphalt rejuvenated with various bio-oils based on rheological property index, J. Clean. Prod. 385 (2023), 135593.
[9] G. Guduru, A. Goli, S. Matolia, K. Kuna, Chemical and performance characteristics of rejuvenated bituminous materials with high reclaimed asphalt content, J. Mater. Civ. Eng. 33 (1) (2021) 04020434.
[10] D. Daryaee, M. Habibpour, S. Gulzar, B. Underwood, Combined effect of waste polymer and rejuvenator on performance properties of reclaimed asphalt binder, Constr. Build. Mater. 268 (2021), 121059.
[11] Y. Zhang, M. Ling, F. Kaseer, E. Arambula, R. Lytton, A. Martin, Prediction and evaluation of rutting and moisture susceptibility in rejuvenated asphalt mixtures, J. Clean. Prod. 333 (2022), 129980.
[12] M. Elkashef, J. Podolsky, R. Williams, N. Hernandez, E. Cochran, Using viscosity models to predict the properties of rejuvenated reclaimed asphalt pavement (RAP) binders, Road. Mater. Pavement Des. 20 (S20) (2019) S767–S779.
[13] A. Hohmann, M. Forrester, M. Staver, B. Kuehl, N. Hernandez, R. Williams, E. Cochran, Chemically mediated asphalt rejuvenation via epoxidized vegetable oil derivatives for sustainable pavements, Fuel 355 (2024), 129374.
[14] M. Ansari, K. Khatri, R. Vishnu, V. Chowdary, Performance evaluation of rejuvenated recycled asphalt blends at high and intermediate pavement temperatures, Int. J. Pavement Eng. 23 (12) (2022) 4112–4124.
[15] M. Elkashef, R. Williams, E. Cochran, Thermal and cold flow properties of bio-derived rejuvenators and their impact on the properties of rejuvenated asphalt binders, Thermochim. Acta 671 (2019) 48–53.
[16] L. Zhang, I. Hoff, X. Zhang, C. Yang, Investigation of the self-healing and rejuvenating properties of aged asphalt mixture containing multi-cavity Ca-alginate capsules, Constr. Build. Mater. 361 (2022), 129685.
[17] H. Zhang, Z. Chen, G. Xu, C. Shi, Evaluation of aging behaviors of asphalt binders through different rheological indices, Fuel 221 (2018) 78–88.
[18] S. Kabir, E. Fini, Investigating aging and rejuvenation mechanism of biomodified rubberized bitumen, J. Mater. Civ. Eng. 33 (7) (2021) 04021142.
[19] D. Oldham, A. Rajib, K. Dandamudi, Y. Liu, S. Deng, E. Fini, Transesterification of waste cooking oil to produce a sustainable rejuvenator for aged asphalt, Resour., Conserv. Recycl. 168 (2021), 105297.
[20] L. Rzek, M. Tusar, L. Perse, Modelling rheological characteristics of rejuvenated aged bitumen, Int. J. Pavement Eng. 23 (4) (2022) 1282–1294.
[21] W. Zeiada, H. Liu, G. Al-Khateeb, A. Shanableh, M. Samarai, Evaluation of test methods for measurement of zero shear viscosity (ZSV) of asphalt binders, Constr. Build. Mater. 325 (2022), 126794.

[22] A. Behnood, Application of rejuvenators to improve the rheological and mechanical properties of asphalt binders and mixtures: a review, J. Clean. Prod. 231 (2019) 171–182.
[23] M. Zahoor, S. Nizamuddin, S. Madapusi, F. Giustozzi, Sustainable asphalt rejuvenation using waste cooking oil: a comprehensive review, J. Clean. Prod. 278 (2021), 123304.
[24] H. Liu, W. Zeiada, G. Al-Khateeb, A. Shanableh, M. Samarai, Characterization of the shear-thinning behavior of asphalt binders with consideration of yield stress, Mater. Struct. 53 (2020) 105.
[25] Y. Wang, K. Zhao, F. Li, Q. Gao, K. Lai, Asphaltenes in asphalt: direct observation and evaluation of their impacts on asphalt properties, Constr. Build. Mater. 271 (2021), 121862.
[26] P. Hajikarimi, M. Rahi, F. Nejad, Comparing different rutting specification parameters using high temperature characteristics of rubber-modified asphalt binders, Road. Mater. Pavement Des. 16 (4) (2015) 751–766.
[27] F. Dong, X. Yu, B. Xu, T. Wang, Comparison of high temperature performance and microstructure for foamed WMA and HMA with RAP binder, Constr. Build. Mater. 134 (2017) 594–601.
[28] K. Zhang, F. Huchet, A. Hobbs, A review of thermal processes in the production and their influences on performance of asphalt mixtures with reclaimed asphalt pavement (RAP), Constr. Build. Mater. 206 (2019) 609–619.
[29] S. Ren, X. Liu, W. Fan, C. Qian, G. Nan, S. Erkens, Investigating the effects of waste oil and styrene-butadiene rubber on restoring and improving the viscoelastic, compatibility, and aging properties of aged asphalt, Constr. Build. Mater. 269 (2021), 121338.
[30] L. Porot, J. Zhu, D. Wang, A. Falchetto, Multiple stress creep recovery test to differentiate polymer modified bitumen at high temperature, J. Test. Eval. (2022), https://doi.org/10.1520/JTE20220306.
[31] G. Skronka, M. Blascik, O. Vacin, M. Jasso, Impact of shear stress levels on validity of MSCR tests. Road materials and pavement, Materials (2022) 2106293.
[32] A. Sharma, G. Naga, P. Kumar, S. Raha, Rheological characterization of recycled asphalt binders and correlating the zero shear viscosity to the Superpave rutting parameter, J. Mater. Civ. Eng. 34 (9) (2022) 04022218.
[33] ASTM D7343. Standard practice for optimization, sample handling, calibration, and validation of X-ray fluorescence spectrometry methods for elemental analysis of petroleum products and lubricants.
[34] Ncat. NCAT researchers explore multiple user of rejuvenators asphalt technology news. 2014, 26(1), 1–16.
[35] EN 15326. British standard for bitumen and bituminous binders-measurement of density and specify gravity-capillary-stoppered pycnometer method.
[36] ASTM D35. Standard test method for penetration of bituminous materials.
[37] ASTM D36. Standard test method for softening point of bitumen (ring and ball apparatus).
[38] AASHTO T316. Standard method of test for viscosity determination of asphalt binder using rotational viscometer.
[39] ASTM D4121. Standard test method for separation of asphalt into four fractions.
[40] S. Ren, X. Liu, P. Lin, R. Jing, S. Erkens, Toward the long-term aging influence and novel reaction kinetics models of bitumen, Int. J. Pavement Eng. (2021) 2024188.
[41] G. Li, Y. Tan, Y. Fu, P. Liu, C. Fu, M. Oeser, Density, zero shear viscosity and microstructure analysis of asphalt binder using molecular dynamics simulation, Constr. Build. Mater. 345 (2022), 128332.
[42] S. Ren, X. Liu, H. Wang, W. Fan, S. Erkens, Evaluation of rheological behaviors and anti-aging properties of recycled asphalts using low-viscosity asphalt and polymers, J. Clean. Prod. 253 (2020), 120048.
[43] Y. Zhang, C. Si, T. Fan, Y. Zhu, S. Li, S. Ren, P. Lin, Research on the optimal dosage of bio-oil/lignin composite modified asphalt based on rheological and anti-aging properties, Constr. Build. Mater. 389 (2023), 131796.
[44] F. Kaseer, A. Martin, E. Arambula-Mercado, Use of recycling agents in asphalt mixtures with high recycled materials contents in the United States: A literature review, Constr. Build. Mater. 211 (2019) 974–987.
[45] C. Wang, L. Song, G. Sun, Comparison and correlation between polymer modified asphalt binders and mastics in high- and intermediate-temperature rheological behaviors, Constr. Build. Mater. 364 (2023), 129963.
[46] M. Gajewski, W. Bankowski, B. Gajewska, D. Sybilski, R. Horodecka, Estimation of asphalt binders' resistance to permanent deformation with application of the MSCR and multiple shear creep long recovery (MSCLR) tests, Constr. Build. Mater. 284 (2021), 122808.
[47] H. Liu, W. Zeiada, G. Al-Khateeb, A. Shanableh, M. Samarai, Use of the multiple stress creep recovery (MSCR) test to characterize the rutting potential of asphalt binders: a literature review, Constr. Build. Mater. (2021), 121320.